

A NOVEL SYNTHESIS OF BENZOXAZOLONE AND DERIVATIVES VIA A RING  
EXPANSION AND REDUCTION APPROACH

A THESIS SUBMITTED TO THE FACULTY OF THE UNIVERSITY OF  
MINNESOTA BY

MARK DELONG

IN PARTIAL FULFILLMENT OF THE REQUIREMENTS FOR THE DEGREE OF  
CHEMISTRY MASTER OF SCIENCE

ADVISOR: DR. PETER GRUNDT

JULY 2022

Copyright

Mark DeLong

2022

All Rights Reserved.

Table of Contents

List of Tables .....ii

List of Figures ..... iii

Introduction.....1

Results and Discussion .....3

Spectroscopy Analysis ..... 17

Conclusion ..... 67

Materials and Methods..... 68

Bibliography ..... 71

Appendix..... 72

Spectroscopy Data ..... 72

## List of Tables

Table 1. Effects of solvent on yield.	5
Table 2. Effects of reagent selection on yields.	6
Table 3. Effects of reagent selection on yields.	6
Table 4. Yields of various derivatives synthesized.	9
Table 5. List and Structures of alternative starting materials tested.	16
Table 6. Table of MS values for compound 1.	18
Table 7. List of observed HSQC interactions.	27
Table 8. List of the most intense interactions in the HMBC.	30
Table 9. $^1\text{H}$ $^{13}\text{C}$ HSQC data for Compound 1.	72
Table 10. $^1\text{H}$ $^{13}\text{C}$ HMBC data for Compound 1.	72
Table 11. COSY data for Compound 1.	72
Table 12. $^1\text{H}$ $^{15}\text{N}$ HMBC data for Compound 1.	72
Table 13. NOESY data for Compound 1.	73
Table 14. $^1\text{H}$ $^{13}\text{C}$ HSQC data for Compound 8.	74
Table 15. $^1\text{H}$ $^{13}\text{C}$ HMBC data for Compound 8.	74
Table 16. COSY data for Compound 8.	74
Table 17. $^1\text{H}$ $^{15}\text{N}$ HMBC data for Compound 8.	75

## List of Figures

Figure 1. Structure of Benzoxazolone.	1
Figure 2. Typical reaction scheme for benzoxazolone and some structures of relevant compounds.	2
Figure 3. Initial reaction scheme.	3
Figure 4. Reaction scheme that gives pure benzoxazolone.	4
Figure 5. Overall synthesis scheme for benzoxazolone derivatives.	8
Figure 6. Numbering used to describe positions in benzoxazolone in this work.	9
Figure 7. Proposed Mechanism.	13
Figure 8. Proposed mechanism for the change in regioselectivity during the initial Baeyer-Villiger oxidation.	14
Figure 9. Total ion chromatogram (TIC) (x-axis corresponds to retention time in seconds) and Mass spectra (x-axis corresponds to m/z) for compound 1.	18
Figure 10. Full $^1\text{H}$ NMR spectrum for compound 1.	19
Figure 11. Aromatic Region of $^1\text{H}$ NMR Spectrum for compound 1.	20
Figure 12. Full $^{13}\text{C}$ NMR spectrum for compound 1.	21
Figure 13. Expanded $^{13}\text{C}$ NMR spectrum for compound 1.	21
Figure 14. Partial NMR assignment of compound 1.	22
Figure 15. Full COSY NMR Spectrum for compound 1.	23
Figure 16. COSY NMR Spectrum aromatic region for compound 1.	23
Figure 17. Full COSY Spectrum with the floor lowered to see additional signals, such as 2 and 4 bond interactions.	24

Figure 18. COSY Spectrum with the floor lowered to see additional signals.	24
Figure 19. Full NOESY Spectrum for compound 1.	25
Figure 20. NOESY spectrum focused on the only signal from the N-H proton.	25
Figure 21. Partial NMR assignment of compound 1 following NOESY and COSY analysis.	26
Figure 22. Full HSQC spectrum for compound 1.	27
Figure 23. Aromatic region of HSQC for compound 1.	28
Figure 24. Partial assignment for compound 1 following HSQC analysis.	29
Figure 25. Full HMBC Spectrum for compound 1.	29
Figure 26. Aromatic Region of HMBC Spectrum for compound 1.	30
Figure 27. Full Assignment of compound 1.	31
Figure 28. Full HMBC Spectrum with raised floor to see weaker interactions.	32
Figure 29. Full HMBC Spectrum with raised floor to see weaker interactions.	33
Figure 30. Full $^1\text{H}$ - $^{15}\text{N}$ HMBC Spectrum for compound 1.	34
Figure 31. $^1\text{H}$ - $^{15}\text{N}$ HMBC Spectrum focused on the only available signal.	34
Figure 32. Full $^1\text{H}$ NMR Spectrum for compound 2.	35
Figure 33. Aromatic region of $^1\text{H}$ NMR spectrum.	36
Figure 34. Full $^{13}\text{C}$ NMR Spectrum for compound 2.	37
Figure 35. Full $^1\text{H}$ Spectrum for compound 3. Peak around 4 ppm is due to water.	38
Figure 36. Aromatic region of $^1\text{H}$ Spectrum for compound 3.	38
Figure 37. Full $^{13}\text{C}$ Spectrum for compound 3.	39
Figure 38. Full $^1\text{H}$ Spectrum for compound 4. Signal at 3.34 ppm is due to water.	40

Figure 39. Aromatic region of $^1\text{H}$ Spectrum for compound 4.	41
Figure 40. Full $^{13}\text{C}$ Spectrum for compound 4.	42
Figure 41. Zoomed in $^{13}\text{C}$ Spectrum for compound 4.	42
Figure 42. Full $^1\text{H}$ Spectrum for compound 5.	43
Figure 43. Aromatic region of $^1\text{H}$ Spectrum for compound 5.	44
Figure 44. Full $^{13}\text{C}$ Spectrum for compound 5.	45
Figure 45. Full $^1\text{H}$ Spectrum for compound 6.	46
Figure 46. Aromatic region of $^1\text{H}$ Spectrum for compound 6.	46
Figure 47. Full $^{13}\text{C}$ Spectrum for compound 6.	47
Figure 48. Full $^1\text{H}$ Spectrum for compound 7.	48
Figure 49. Aromatic Region of $^1\text{H}$ Spectrum for compound 7.	48
Figure 50. Full $^{13}\text{C}$ Spectrum for compound 7.	49
Figure 51. Full $^1\text{H}$ Spectrum for compound 8.	50
Figure 52. Aromatic region of $^1\text{H}$ Spectrum for compound 8.	51
Figure 53. Full $^{13}\text{C}$ Spectrum for compound 8.	52
Figure 54. Full $^1\text{H}$ Spectrum for compound 9.	53
Figure 55. Alkyl region of $^1\text{H}$ Spectrum for compound 9.	53
Figure 56. Aromatic region of $^1\text{H}$ Spectrum for compound 9.	54
Figure 57. Full $^{13}\text{C}$ Spectrum for compound 9.	55
Figure 58. Full $^1\text{H}$ Spectrum for compound 10.	56
Figure 59. Aromatic region of $^1\text{H}$ Spectrum for compound 10.	56
Figure 60. Full $^{13}\text{C}$ Spectrum for compound 10.	57

Figure 61. Total ion chromatogram for compound 10.	58
Figure 62. Mass spectrum for the largest peak in the TIC.	59
Figure 63. Mass spectrum for the second largest peak in the TIC.	60
Figure 64. Mass spectrum for the third largest peak in the TIC.	61
Figure 65. Full $^1\text{H}$ Spectrum for compound 11.	62
Figure 66. Aromatic region of $^1\text{H}$ Spectrum for compound 11.	63
Figure 67. Full $^{13}\text{C}$ Spectrum for compound 11.	64
Figure 68. Total ion chromatogram for compound 11.	65
Figure 69. Mass Spectrum for the largest peak in the TIC.	65
Figure 70. Mass spectrum for the second largest peak in the TIC.	66



## Introduction

Benzoxazolone (Figure 1) is a heterocyclic aromatic molecule with numerous applications across several fields, such as medicine and materials science. The structure of benzoxazolone is a very important biologically active moiety that gives rise to compounds

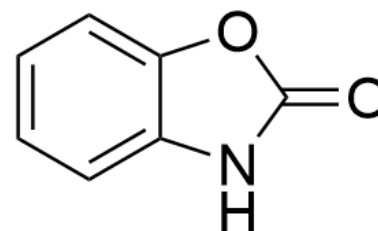


Figure 1. Structure of Benzoxazolone.

with an extremely wide array of activities. Ucar, et al. note that benzoxazolone derivatives to exhibit antiepileptic, analgesic, anti-inflammatory- antispasmodic, antitubercular, antibacterial, antimicrobial, antifungal, and normolipemic activities (1998). Similarly, Soyer et al. (2014) note the following activities: analgesic, anticonvulsant, dopaminergic, anti-HIV, antinociceptive, and antimalarial. The compound benzoxazole, which is very structurally similar and has been researched more, has been found to have the following activities: Antibacterial, antifungal, anticancer, anti-inflammatory, antimycobacterial, antihistamine, antiparkinson's, inhibition of hepatitis C virus, 5-HT<sub>3</sub> antagonistic effect, melatonin receptor antagonism, amyloidogenesis inhibition and Rho-kinase inhibition (Kakkar et al., 2018).

In addition, Hwang et al. found chromophore applications for benzoxazole derivatives for use in computers and lasers. Without a doubt it can be said that these are very versatile compounds hold huge potential to many different fields of research.

Currently in the literature there are a few routes of synthesis for benzoxazolone and its derivatives. Most start from 2-aminophenol derivatives (Figure 1) and involve various reaction schemes. Perhaps the most common route of synthesis uses carbonyl diimidazole

and 2-aminophenol to give benzoxazolone, a reaction reported by Nachman, R. in 1982. Another route of synthesis includes condensing 2-aminophenol with urea at high temperatures (Varma et al., 1977). These are the two

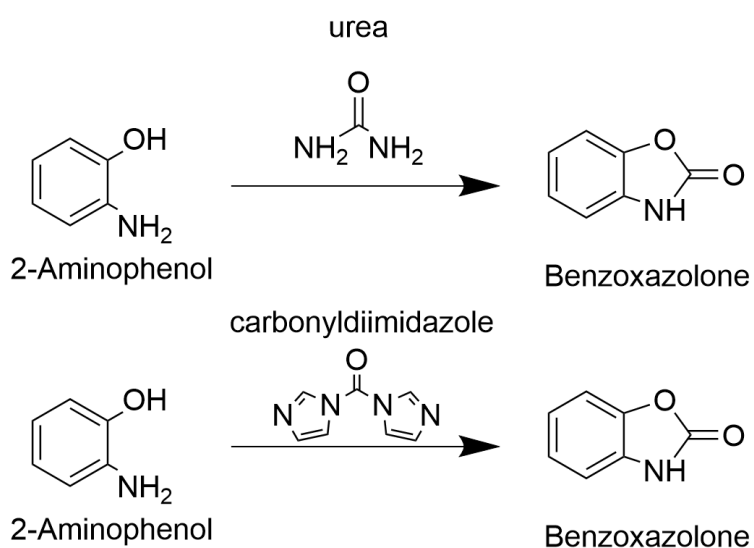


Figure 2. Typical reaction scheme for benzoxazolone and some structures of relevant compounds.

main routes of synthesis seen in the literature, but there are some other new routes of synthesis used by other groups. Most of the new routes still use 2-aminophenol as the starting material, utilize multiple steps, and require various catalysts. This can make for inconvenient, multistep syntheses that use expensive reagents and can have negative environmental impacts. The route of synthesis of benzoxazolone from 2-aminophenol seems optimal, however to the best of our knowledge no one has shown that a wide selection of benzoxazolone derivatives can be made using that method. Therefore, the area of benzoxazolone synthesis could benefit from some new synthetic methods.

In this work, we describe a serendipitous discovery for a new route of synthesis for benzoxazolone and derivatives using a very simple reaction system, and one that allows access to benzoxazolone from different starting materials.

This project has its origins during my work as an undergraduate student. At first, we put together the following reaction in an attempt to create iodinated isatoic anhydride derivatives, which would later be used to create medicinal compounds.



Figure 3. Initial reaction scheme.

However, after characterizing the product, we found a mixture of compounds, and after performing further analysis we found the unexpected product to be benzoxazolone (Compound 1). However, the yields were low, and the purity was low as well since there were multiple products in the mixture. This is where my Master's work began. My goal was to optimize this reaction to get benzoxazolone in higher purity and yield and synthesize multiple derivatives as many of substituted benzoxazolones demonstrate very important properties.

### **Results and Discussion**

Since we knew that isatin oxidizes to isatoic anhydride in the presence of oxone readily, we hypothesized that perhaps benzoxazolone was a product of isatoic anhydride reacting further with iodide and oxone to form benzoxazolone. This was not the case upon further testing. This then meant that we had competing reactions, where anytime isatin converted

into isatoic anhydride, that would take away yield from the reaction that converts to benzoxazolone. With that in mind, we tried various starting materials until we met success with 2H-1,4-Benzoxazine-2,3(4H)-dione.

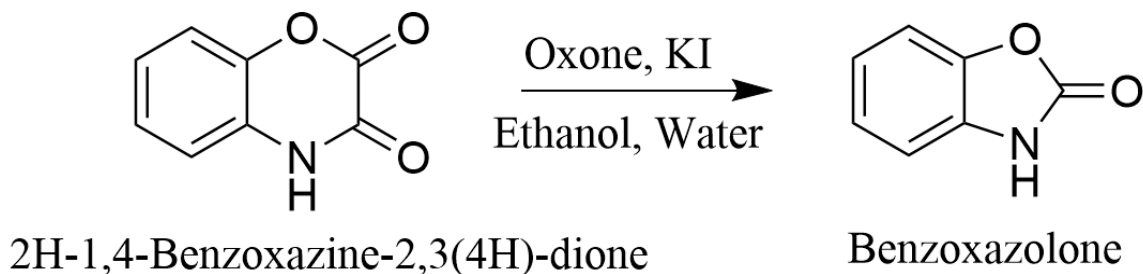


Figure 4. Reaction scheme that gives pure benzoxazolone.

This reaction proved to give benzoxazolone as the sole product. This likely means that for some reason unknown to us, the presence of iodide changes the position the oxygen is inserted into isatin; normally it is inserted in between the carbonyls to give isatoic anhydride, however in the presence of iodide it is inserted to the side of them. This will be discussed again in the mechanism section.

At this point however we realized that we have a new route of synthesis for the important molecule benzoxazolone as well as some derivatives potentially. Therefore, we moved our efforts into optimizing this reaction and synthesizing derivatives.

### Optimization and Derivatives

Various reaction conditions were explored to optimize the yield and purity of this reaction, as well as possibly uncover some aspects of its mechanism. First the impacts on yield were examined, and the results are compiled below in Table 1.

Table 1. Effects of solvent on yield. Reaction conditions are 3 eq. of Oxone and 0.1 eq. of KI.

Solvent	Yield (%)
EtOH:H <sub>2</sub> O 1:3	54
CH <sub>3</sub> CN:H <sub>2</sub> O 1:3	80
CH <sub>3</sub> CN:H <sub>2</sub> O 3:1	50
CH <sub>3</sub> CN	0
AcOH:H <sub>2</sub> O 1:3	66
DMF:H <sub>2</sub> O 1:3	50
Toluene:H <sub>2</sub> O 1:3	62
H <sub>2</sub> O	54

The optimal solvent for these reaction conditions appears to be a 1:3 ratio of acetonitrile and water, giving about 80% yield, while other similar combinations tend to give lower yields around 50-60%. There are two other data points here that are important to examine, and that is when we use only water and only organic solvent. In the case of using only organic solvent, the yield drops to 0%, suggesting these reaction conditions need some amount of water. Whether that is due to the nature of the reaction mechanism, or the need for some reagents to be dissolved (i.e. Oxone) cannot be determined from this data alone. When using water only as the solvent, the yield remains moderate, at 54%. Using only water as a solvent is convenient, however it is not useful when nearly any other derivative is tested, as most derivatives of these compounds are insoluble in water, which results in a drastically reduced yield and purity.

Next the effect of various reagents and amounts of those reagents on the yield were compiled below.

Table 2. Effects of reagent selection on yields. Reaction conditions are assumed to be 0.1 eq. KI, 3 eq. Oxone, and 3:1 H<sub>2</sub>O:CH<sub>3</sub>CN, but they are modified as noted.

Reactant	Yield (%)
0.1 eq. Potassium Iodide	80
1 eq. Potassium Iodide	67
3 eq. Potassium Iodide	<10
0 eq. Oxone	0
0.1 eq. Oxone	0
1.2 eq. Oxone	62
3 eq. Oxone	79

Table 3. Effects of reagent selection on yields. Reaction conditions below were performed with only the specified reagents in a 3:1 H<sub>2</sub>O:CH<sub>3</sub>CN solvent system.

Reactant	Yield (%)
1 eq. Iodine and 3 eq. Oxone	30
0.1 eq. Potassium Periodate	<10
1 eq. Potassium Periodate	80
2 eq. Potassium Periodate	77
1 eq. Potassium Permanganate	13
1 eq. Potassium Permanganate and 1 eq. Potassium Iodide	21

0.1 eq. Potassium Bromide and 3 eq. Oxone	0
3 eq. Potassium Bromide and 3 eq. Oxone	0

From the data given in two above tables, it becomes apparent that there are two effective reagent selections that give the product, that is a mixture of 0.1 eq. KI and 3 eq. Oxone, or just 1 eq. of potassium periodate. Both gave about 80% yield. It should be noted that just using iodide without Oxone does not give any conversion to product and using just Oxone without potassium iodide does not give significant conversion to the product, however benzoxazolone can be detected in the NMR.

Regarding the amounts of potassium iodide used in these reactions, it appears that it is only required in a catalytic amount, and in fact that provides the best yield. This has strong implications for the type of mechanism involved in this reaction, as the active iodine species must get regenerated somehow throughout the course of the reaction. Using larger amounts actually decreases the yield, because the excess iodine actually goes on to iodinate the product, resulting in a diiodo benzoxazolone compound. This is likely due to the formation of electrophilic iodine species when iodine interacts with Oxone, which is well documented in the literature (Narender et al.). Interestingly, potassium bromide was also tested to see if the reaction would proceed and yields were not obtained using catalytic amounts, but if a large excess was added then brominated benzoxazolone compounds would form. From this information, it appears that some sort

of active bromide species is also capable of driving this reaction forward, however it appears to be less efficient than using iodide.

Potassium periodate alone is capable of driving this reaction forward when one equivalent is used, which makes for a really convenient reaction system. This reagent was tested because it seemed reasonable that mixing iodide with an oxidizer such as Oxone may produce potassium periodate, which could be the identity of the active species catalyzing this reaction. While we still do not know if this is the species formed *in situ*, it is capable of driving the reaction forward with great efficiency. This also has implications for the reaction mechanism that will be discussed later.

Since it was discovered that potassium periodate is a great reagent for moving this reaction forward another similar reagent, potassium permanganate, was also tested, however it only gave low yields.

With the reaction conditions optimized, we tested if these reaction conditions could be used to produce various derivatives. Different derivatives of 2H-1,4-Benzoxazine-2,3(4H)-dione, the starting material, were created according to the following reaction scheme (Figure 5).

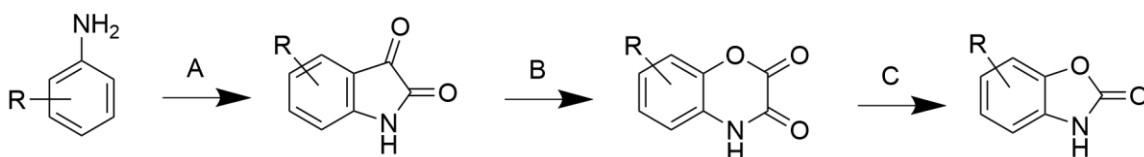


Figure 5. Overall synthesis scheme for benzoxazolone derivatives. Reaction A: 1. Hydroxylamine•HCl, Chloral Hydrate, Sodium Sulfate, HCl, H<sub>2</sub>O, 55°C, 24 hr. 2. H<sub>2</sub>SO<sub>4</sub> 80°C 30 min. Reaction B: Potassium Persulfate, H<sub>2</sub>SO<sub>4</sub>, 0°C, 1 hr. Reaction C: Current work described below: Oxone, KI, CH<sub>3</sub>CN, H<sub>2</sub>O or KIO<sub>4</sub>, CH<sub>3</sub>CN, H<sub>2</sub>O.



The yields of various derivatives with aromatic substitutions can be seen in the table below. The positions assigned to this molecule can be seen in Figure 6. This will be referenced in the table below and in later NMR analysis.

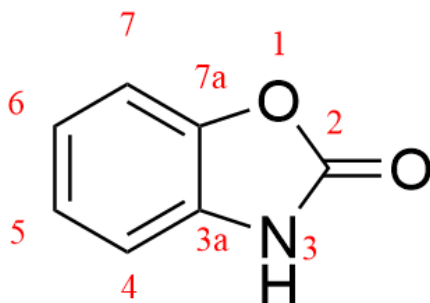
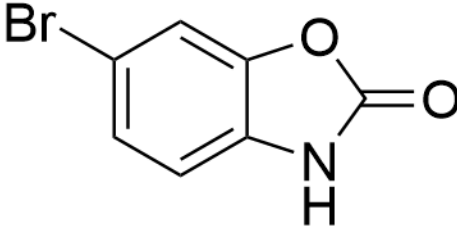
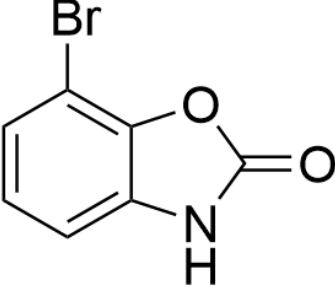
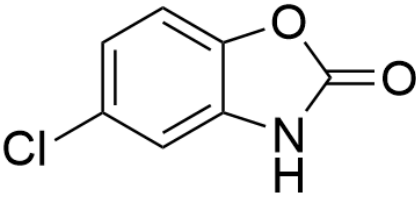
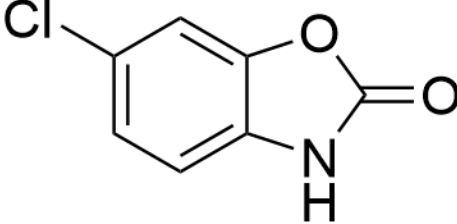
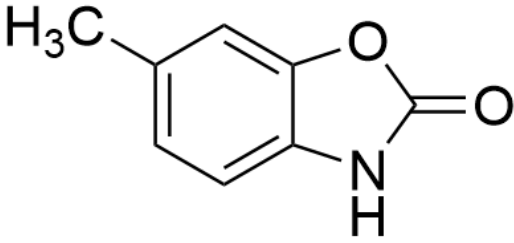
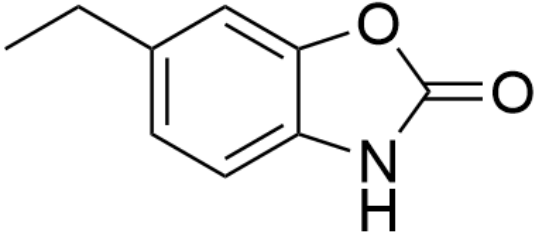
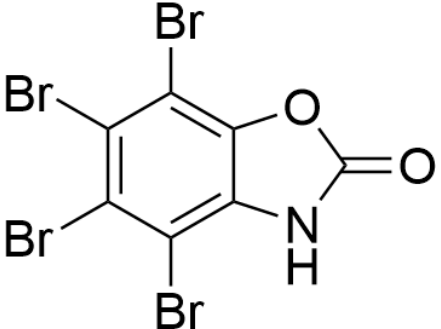
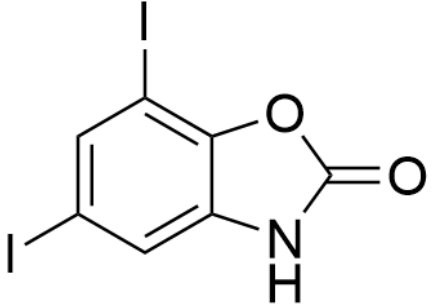


Figure 6. Numbering used to describe positions in benzoxazolone in this work.

Table 4. Yields of various derivatives synthesized. The  $\text{KIO}_4$  reaction method was chosen for all of the derivatives except for compound 11 which used Oxone and excess KI, and compound 10 which used Oxone and excess KBr.

Compound	Structure	Yield (%)
1		80
2		54
3		25

4	 <p>Chemical structure of 4-bromo-1,2,4-oxadiazol-5(1H)-one. It consists of a benzene ring with a bromine atom at the para position (4-position) and a 1,2,4-oxadiazol-5(1H)-one ring system at the 1 and 2 positions of the benzene ring.</p>	63
5	 <p>Chemical structure of 3-bromo-1,2,4-oxadiazol-5(1H)-one. It consists of a benzene ring with a bromine atom at the meta position (3-position) and a 1,2,4-oxadiazol-5(1H)-one ring system at the 1 and 2 positions of the benzene ring.</p>	49
6	 <p>Chemical structure of 3-chloro-1,2,4-oxadiazol-5(1H)-one. It consists of a benzene ring with a chlorine atom at the meta position (3-position) and a 1,2,4-oxadiazol-5(1H)-one ring system at the 1 and 2 positions of the benzene ring.</p>	62
7	 <p>Chemical structure of 4-chloro-1,2,4-oxadiazol-5(1H)-one. It consists of a benzene ring with a chlorine atom at the para position (4-position) and a 1,2,4-oxadiazol-5(1H)-one ring system at the 1 and 2 positions of the benzene ring.</p>	55
8	 <p>Chemical structure of 4-methyl-1,2,4-oxadiazol-5(1H)-one. It consists of a benzene ring with a methyl group (H<sub>3</sub>C) at the para position (4-position) and a 1,2,4-oxadiazol-5(1H)-one ring system at the 1 and 2 positions of the benzene ring.</p>	66
9	 <p>Chemical structure of 4-propyl-1,2,4-oxadiazol-5(1H)-one. It consists of a benzene ring with a propyl group at the para position (4-position) and a 1,2,4-oxadiazol-5(1H)-one ring system at the 1 and 2 positions of the benzene ring.</p>	62

10		60
11		64

Various halogenated derivatives as well as alkyl derivatives can be synthesized using this method in moderate to high yields. In addition, every position seems to be compatible with this route of synthesis, as is shown by fact that a bromo derivative can be acquired regardless of the position desired. In addition, a diiodo benzoxazolone could be acquired with simple reaction conditions which has very limited routes of synthesis in literature. Similarly, compound 10 was acquired which has an aromatic ring saturated with bromines. These compounds could theoretically be used in cross coupling reactions to create various other desired derivatives not described here.

Next, what we have discovered regarding the mechanism of this reaction will be discussed.

### Mechanism

Looking at the reaction scheme, it appears that we lose a carbon and an oxygen in this reaction. The most probable explanation is that CO<sub>2</sub> evolves out of this molecule to lose that carbon and oxygen, which most likely means that the intermediate steps of this reaction result in the ring opening, CO<sub>2</sub> evolving out, and then the ring closing back up again. To the best of our knowledge, this kind of reaction behavior has never been recorded in literature using just potassium periodate or the Oxone/KI system.

Some of the data presented earlier provides us with clues to the kind of reaction mechanism that occurs here. First of all, only a catalytic amount of iodide is needed, so it follows that the active iodide species in this reaction is regenerated somehow. Alone this does not give us much information, but it is something that should be kept in mind.

Next, potassium periodate alone is capable of performing this transformation. While this kind of reaction behavior has not been recorded for this reagent, what is well established is that it participates in glycol or dicarbonyl cleavage. Therefore, we hypothesize that the first step of this reaction may be the carbon-carbon bond breaking in between the two carbonyls when looking at 2H-1,4-Benzoxazine-2,3(4H)-dione. Generally speaking, this is an oxidative reaction that would likely result in the formation of carboxyl groups. If this is the case in this reaction, then that would provide the opportunity for CO<sub>2</sub> to evolve out. Our hypothesized mechanism for these steps can be seen in Figure 7 below.

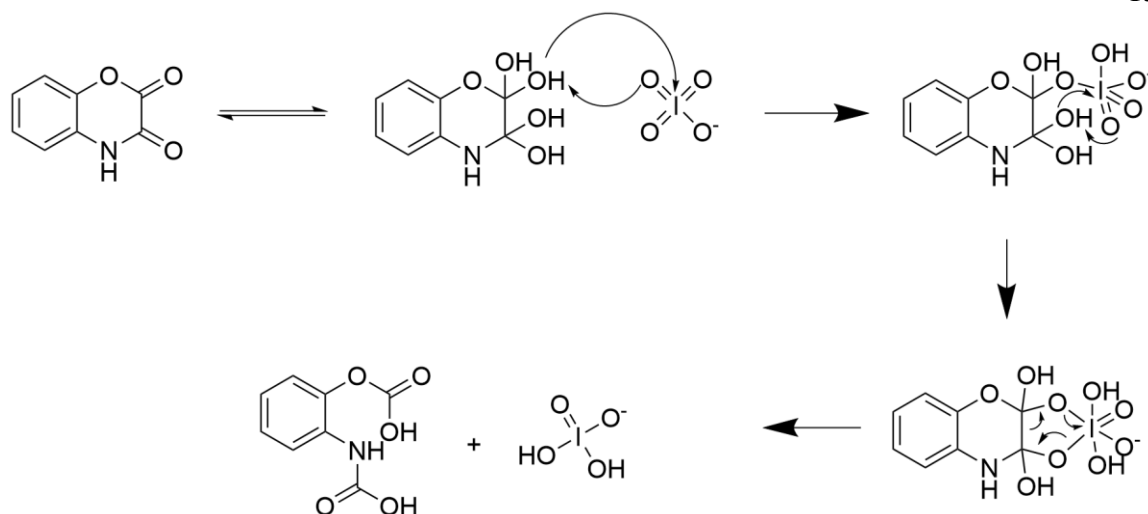


Figure 7. Proposed Mechanism.

The first step involves the equilibrium of carbonyls and their geminal diol form, which happens naturally in aqueous solutions. From the diol form, the reaction with periodate follows as described by the Malaprade reaction mechanism. As mentioned above, by looking at the product at the end of these steps, it seems feasible that a carbon could leave through the evolution of CO<sub>2</sub>, however we are unsure about which carbon leaves and what the mechanism would look like for the cyclization to benzoxazolone.

To help further our understanding of the mechanism we attempted tracking the carbons through heavy isotopes of compounds of 2H-1,4-Benzoxazine-2,3(4H)-dione, however we were unsuccessful due to the difficulty of synthesizing the compounds with a specific carbon isotope on the desired position. We plan on working on this more in the future to acquire more information regarding the mechanism of this reaction.

As discussed before, we observed this reaction initially when we used isatin as the starting material. So, there is some sort of new reaction mechanism that changes the location that the oxygen is inserted into isatin when iodide is present. Normally the

oxygen is inserted in between the carbonyls in isatin to form isatoic anhydride as almost the sole product. However, in the presence of iodide, some 2H-1,4-Benzoxazine-2,3(4H)-dione is formed which goes on to convert into benzoxazolone. This is also intended to be the focus of some future work, as altering the regioselectivity of Baeyer-Villiger reactions could be useful in synthesis, as well as being able to synthesize benzoxazolone directly from isatin derivatives, which are commercially available. Our proposed mechanism for this behavior can be seen in the figure below.

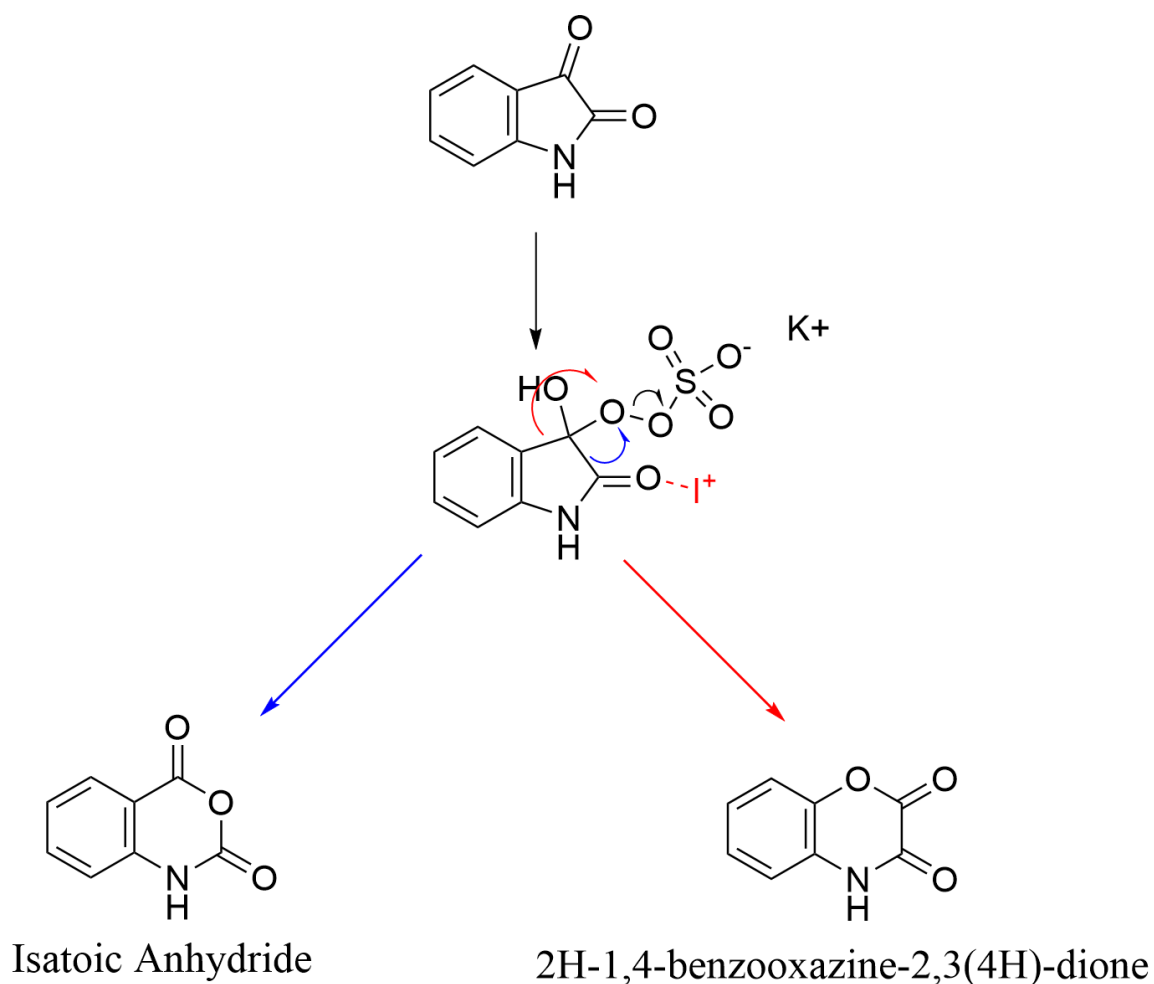


Figure 8. Proposed mechanism for the change in regioselectivity during the initial Baeyer-Villiger oxidation.

In the figure above, two possible electron movements can happen at this key step. Either the electrons in the bond closer to the aromatic ring donate to the peracid oxygen (red), or the electrons in the bond farther from the aromatic ring donate to the peracid oxygen (blue). Without iodine present in the reaction mixture, this regioselectivity is almost entirely shifted to the scheme indicated by the blue arrows. However, the scheme with red arrows demonstrates what we observed during this project. It is well established that the mixture of iodide and oxone produces many different electrophilic species of iodine, including HOI, which readily produces I<sup>+</sup> in solution. It is likely that electrophilic iodine is able to coordinate to the amide carbonyl, and therefore steal electron density from that region in the molecule. This makes the bond on that side more electron poor, and therefore less likely to donate to the incoming oxygen from the oxone, and we would expect to see the reaction highlighted in red occur more often in comparison.

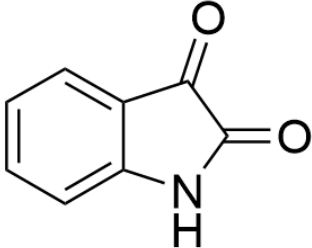
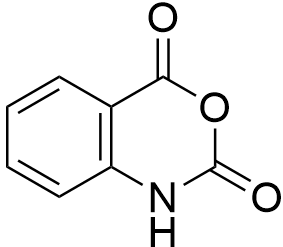
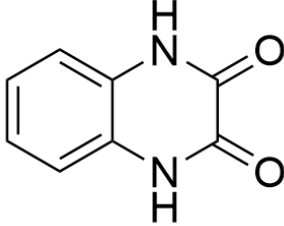
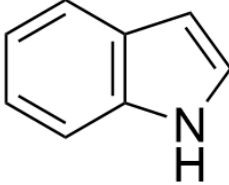
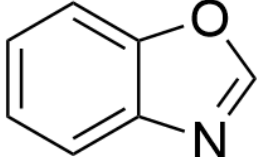
To be clear, this is a hypothesis to explain the phenomena we observed. We do not have explicit data to support this, and it is one of the goals of our future work.

### Different Starting Materials

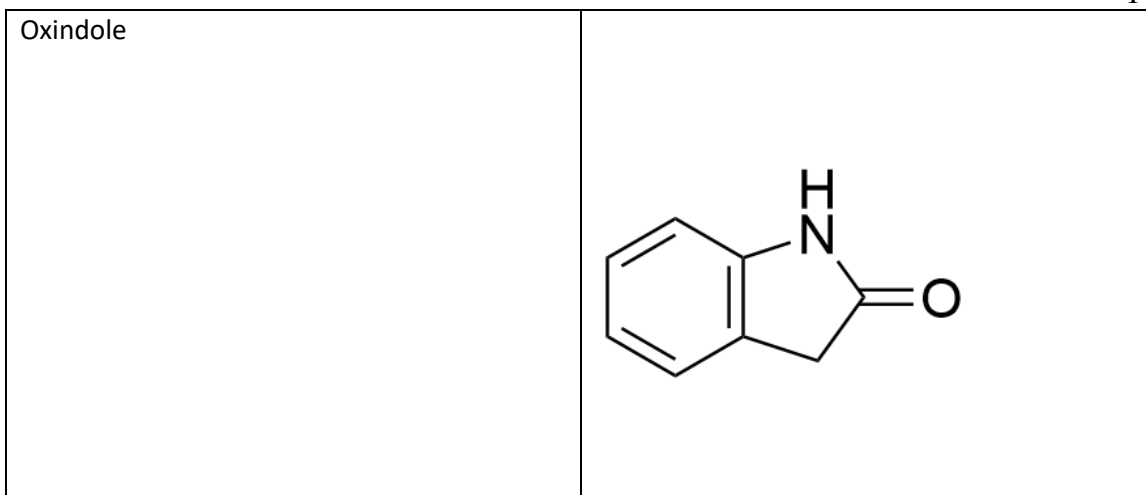
Given that we have a very simple reaction scheme which can shape the chemistry of a cyclic structure, we decided that it would be useful to see if we can perform the same kind of reaction with various other compounds to see if we get a similar conversion. This would help create a more versatile reaction to be used as a tool by organic chemists, and also possibly help us determine parts of the mechanism.

To do this, a variety of compounds were subjected to the same reaction conditions: 3 eq. Oxone, 0.1 eq. KI, and a 3:1 ratio of CH<sub>3</sub>CN:H<sub>2</sub>O. These compounds can be seen below.

Table 5. List and Structures of alternative starting materials tested.

Compound	Structure
Isatin	 <chem>O=C1C(=O)Nc2ccccc12</chem>
Isatoic Anhydride	 <chem>O=C1OC(=O)Nc2ccccc12</chem>
1,4-dihydroquinoxaline-2,3-dione	 <chem>O=C1NC(=O)c2ccccc2N1</chem>
Indole	 <chem>Nc1ccccc2c1c[nH]2</chem>
Benzoxazole	 <chem>c1ccc2c(c1)oc[nH]2</chem>





Overall, none of these compounds gave any meaningful conversion to benzoxazolone or an analogous product. As mentioned previously, isatin does give some conversion to benzoxazolone however it is in low yield and purity. These compounds were all chosen because they have some chemical similarity one way or another to 2H-1,4-Benzoxazine-2,3(4H)-dione, however the reactions did not proceed.

In the next section the characterization of all of the derivatives synthesized in this experiment will be discussed.

### Spectroscopy Analysis

#### Compound 1

To characterize this compound a combination of mass spectrometry as well as various NMR analyses were performed. Below we will start with the data from the mass spectrometry measurements.

Table 6. Table of MS values for compound 1. Only fragments with relative intensities above 15 were included.

Mass/Charge Ratio	Intensity	Relative Intensity
52	385536	27.51
79	611520	43.64
91	241024	17.20
135	1401344	100

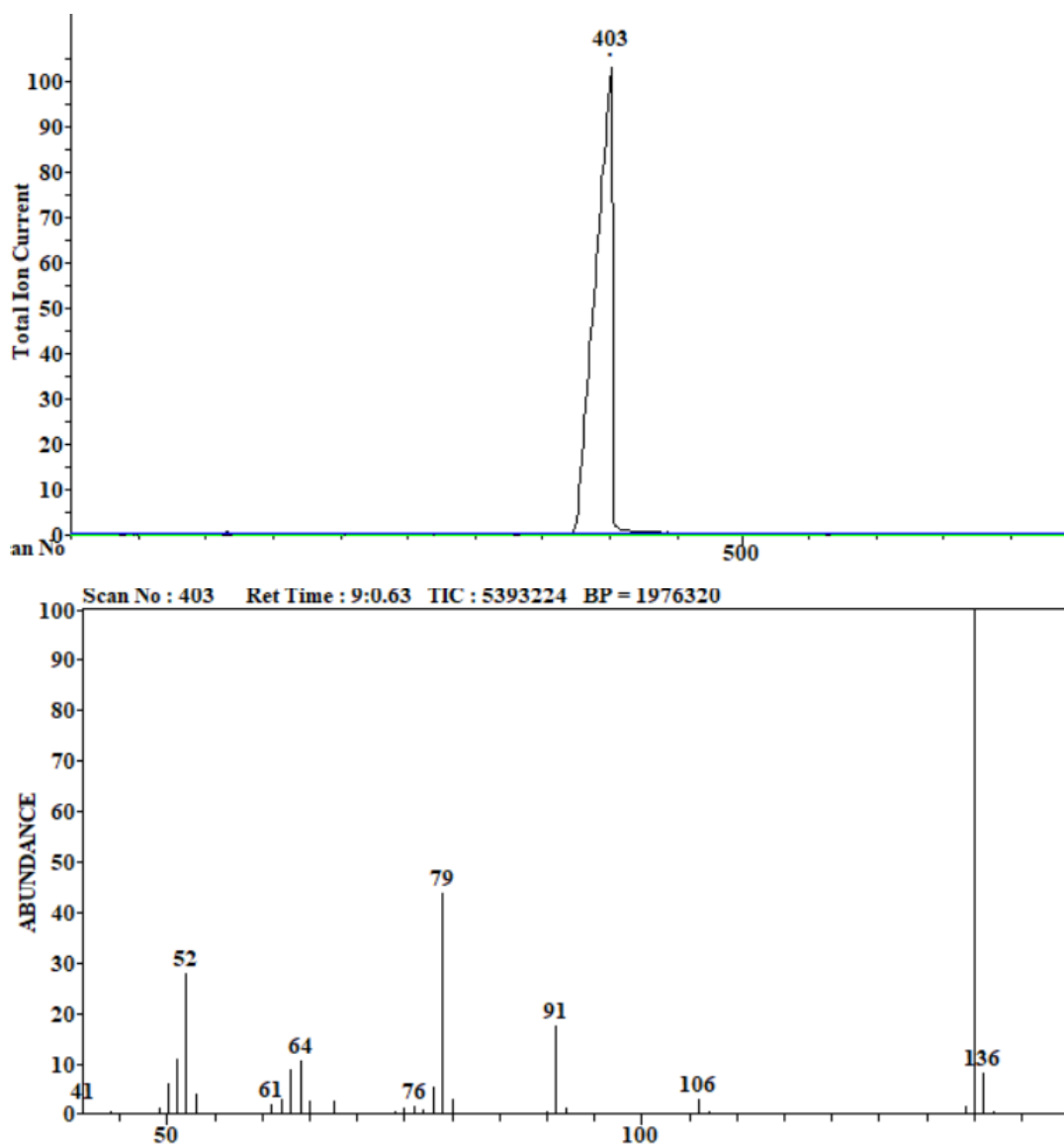


Figure 9. Total ion chromatogram (TIC) (x-axis corresponds to retention time in seconds) and Mass spectra (x-axis corresponds to m/z) for compound 1.

The GC/MS data show a pure sample with a molecular ion of 135, which matches the molecular weight expected for compound 1. Now the rest the structure will be deduced using NMR.

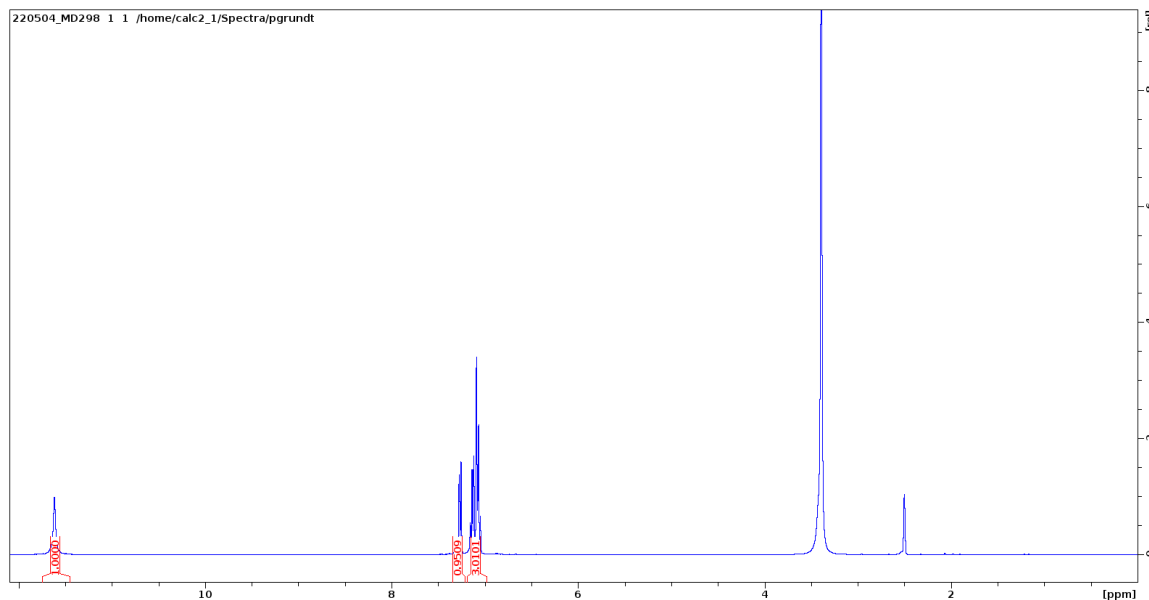


Figure 10. Full  $^1\text{H}$  NMR spectrum for compound 1. NMR Solvent = DMSO- $\text{d}_6$ . Signal at 3.34 is due to water, and the signal at 2.5 is due to DMSO.

From looking at the  $^1\text{H}$  spectrum we can see a highly shifted signal at 11.62 ppm, which belongs to the N-H proton. An integration of signals in the aromatic region of 4H can be seen, which is expected given the structure of the molecule. The aromatic region will be analyzed next.

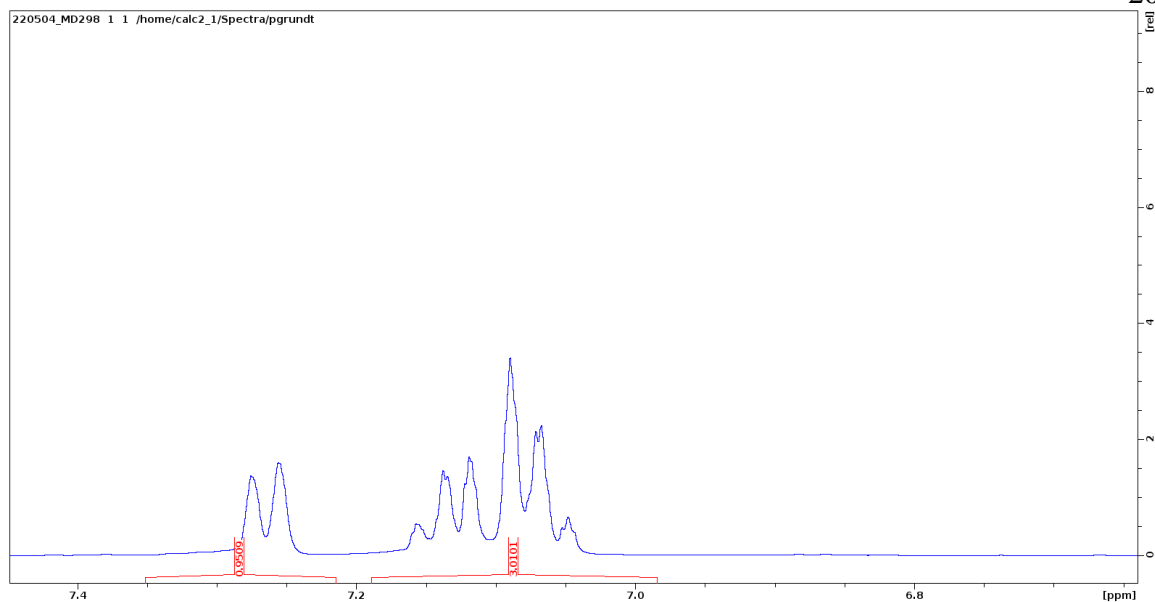


Figure 11. Aromatic Region of  $^1\text{H}$  NMR Spectrum for compound 1.

A clear doublet signal at 7.26 ppm can be seen here. The remaining three aromatic proton signals overlapped in some way to produce the multiplet from 7.03-7.17 ppm. A doublet and two triplets belong to it, however specific chemical shifts cannot be determined from this spectrum alone. This is all the information that can be derived from the proton NMR at the moment. Next the carbon NMR will be analyzed.

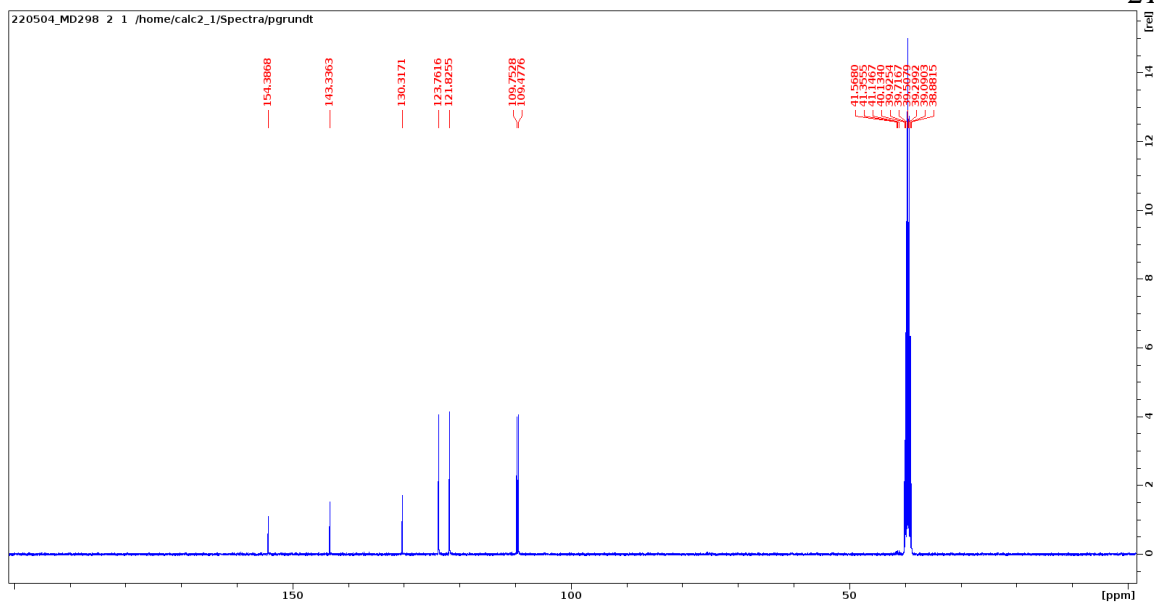


Figure 12. Full  $^{13}\text{C}$  NMR spectrum for compound 1. Signal at 39.51 is due to DMSO.

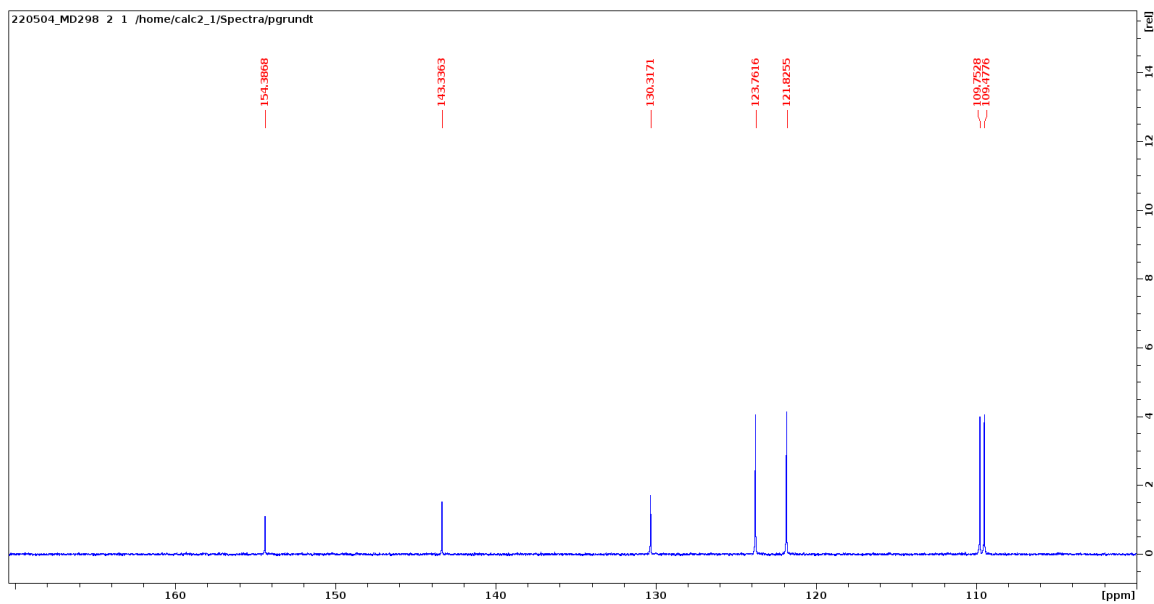


Figure 13. Expanded  $^{13}\text{C}$  NMR spectrum for compound 1. The two signals at 109 ppm can now be discerned.

The  $^{13}\text{C}$  NMR gives seven total signals from the compound, which is expected given the molecule's structure. The highest shifted carbon at 154.9 ppm is assumed to be due to the

amide carbon at this point. This will be reaffirmed with later analysis. The remaining six signals make up the benzene ring.

At this point, two atoms have been assigned which will give us a starting point with the rest of the structural analysis.

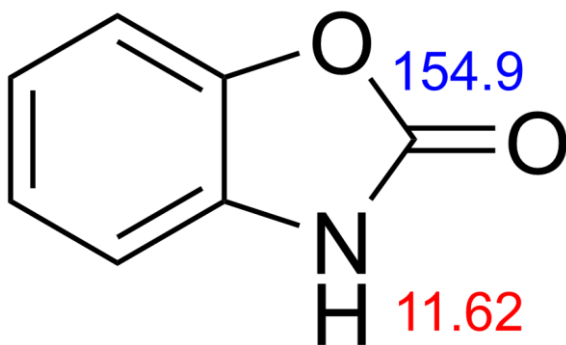


Figure 14. Partial NMR assignment of compound 1. Carbon assignments are in blue. Proton assignments are in red.

The next goal was to assign the identity of at least one of the aromatic protons so the identity of the rest of the ring can be assigned using two-dimensional NMR analysis.

Unfortunately, the three-bond interaction between the N-H proton and the nearby aromatic proton in the 4 position cannot be visualized in the  $^1\text{H}$   $^{13}\text{C}$  HMBC. This remains true for many derivatives of this molecule.

Therefore, the spectra used to access the aromatic ring was the COSY and the NOESY.

The results from them are posted below.

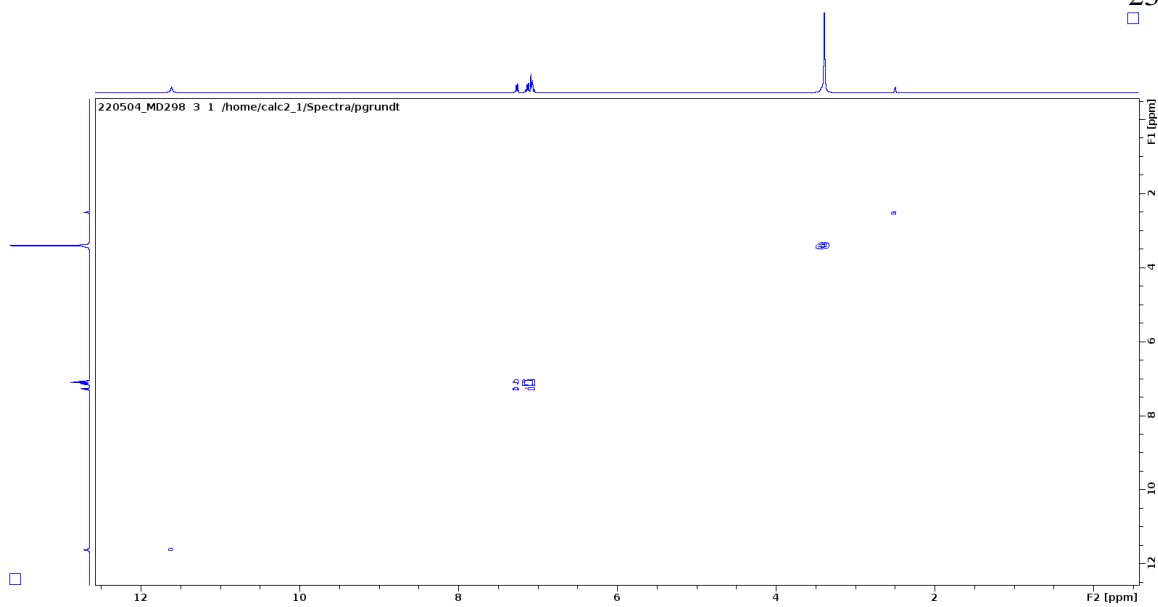


Figure 15. Full COSY NMR Spectrum for compound 1.

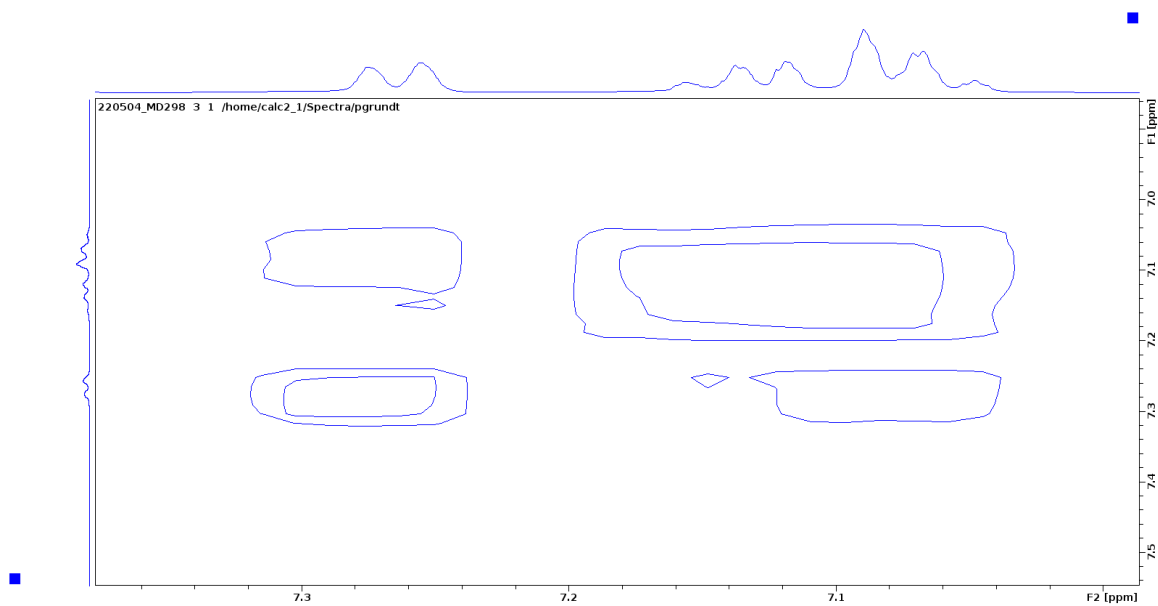


Figure 16. COSY NMR Spectrum aromatic region for compound 1.

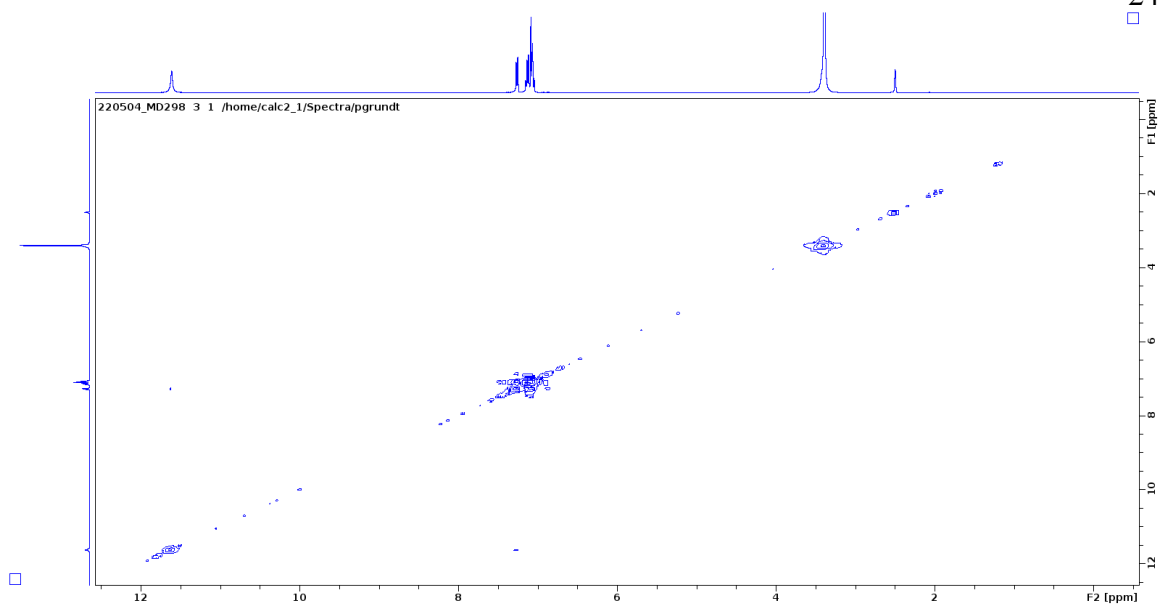


Figure 17. Full COSY Spectrum with the floor lowered to see additional signals, such as 2 and 4 bond interactions.

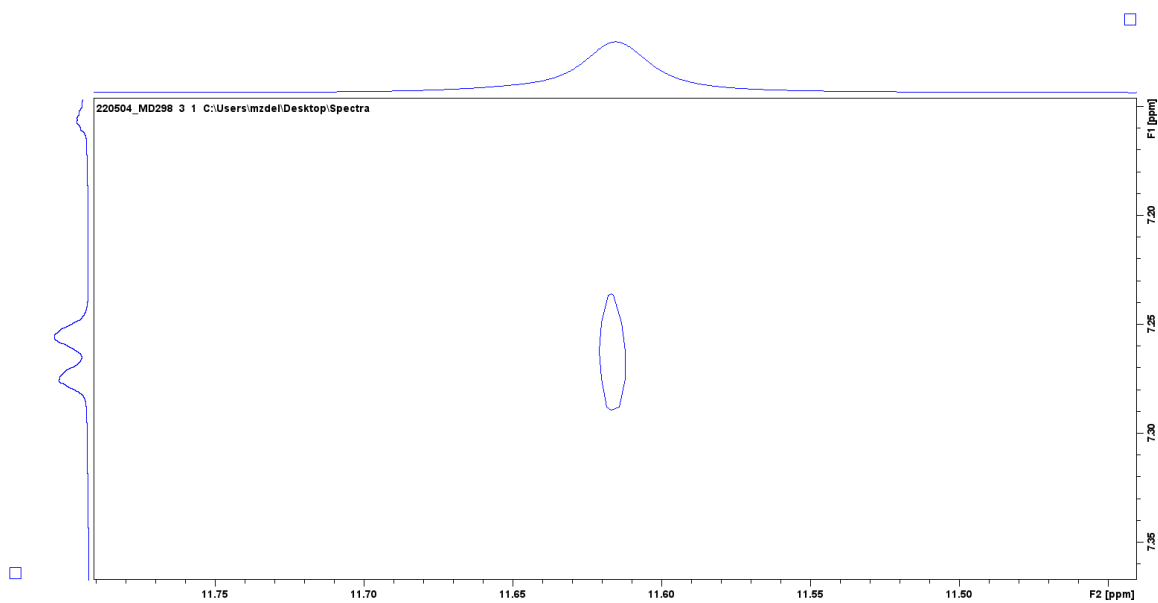


Figure 18. COSY Spectrum with the floor lowered to see additional signals. The signal arising from a 4-bond interaction has been focused.



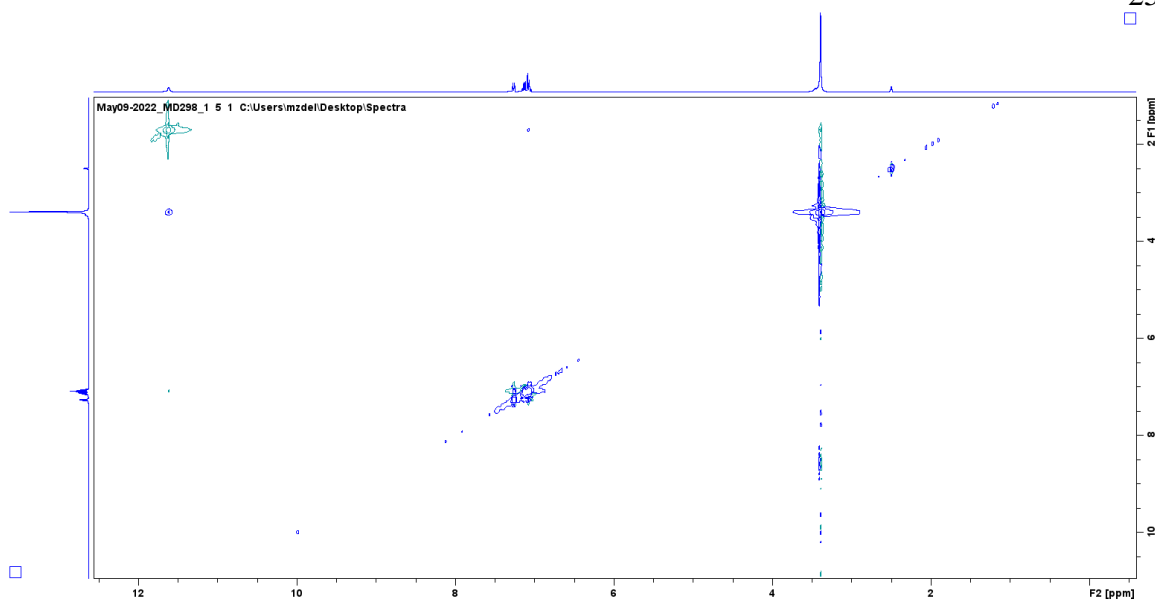


Figure 19. Full NOESY Spectrum for compound 1.

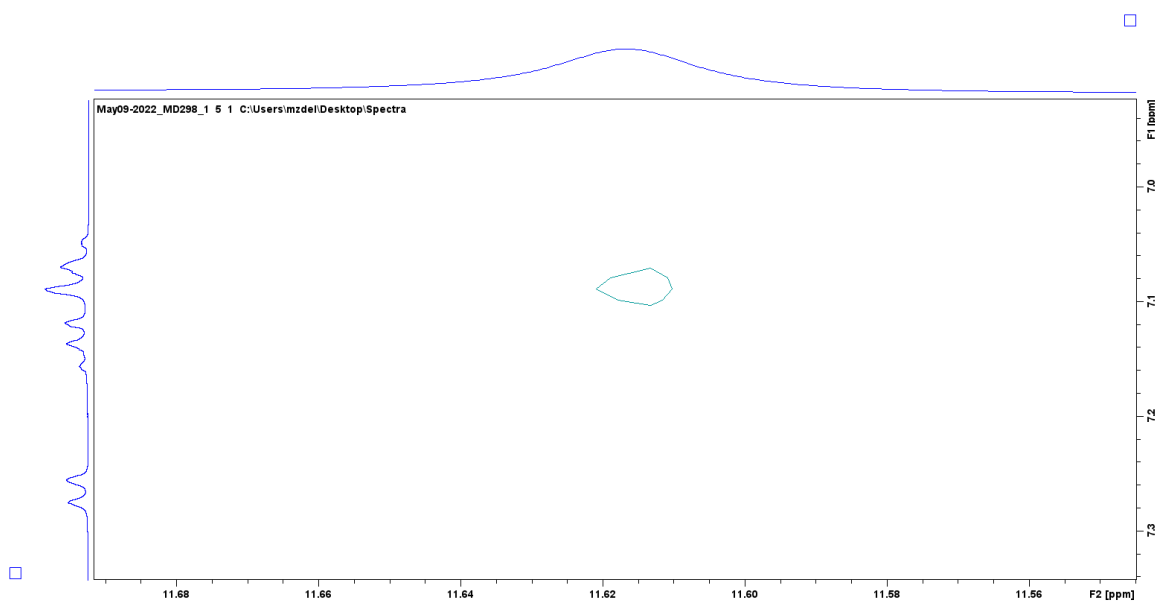


Figure 20. NOESY spectrum focused on the only signal from the N-H proton.

COSY spectra generally show interactions between two hydrogens that are 3-bonds away, which tends to be hydrogens on neighboring carbons, while the NOESY tends to show the interaction between a N-H and a hydrogen that are 3 angstroms away. The most important signal in the COSY can be seen in Figure 18 between the 7.26 ppm doublet and

the 11.63 ppm singlet, while the most important signal in the NOESY can be seen in Figure 20 between the 7.08 ppm and 11.63 ppm signals. We would typically predict that both of these spectra would agree in this situation regarding the identity of the hydrogen in the 4 position; the N-H proton and the H in the 4 position are about 3 angstroms away, and those are 4 bonds away, which can be visualized in COSY, however the signals are usually less intense. However in this situation it seems that there is a disagreement as they are showing interactions with two different hydrogens. The assignment we will proceed with here is following the NOESY, since its signals are much less likely to be distorted, whereas the COSY could easily be displaying a 5-bond interaction with the hydrogen in the 7 position. In fact, with other derivatives of this molecule where there is a substitution in the 7 position, no COSY signals can be obtained. The new assignments will be made and can be seen below.

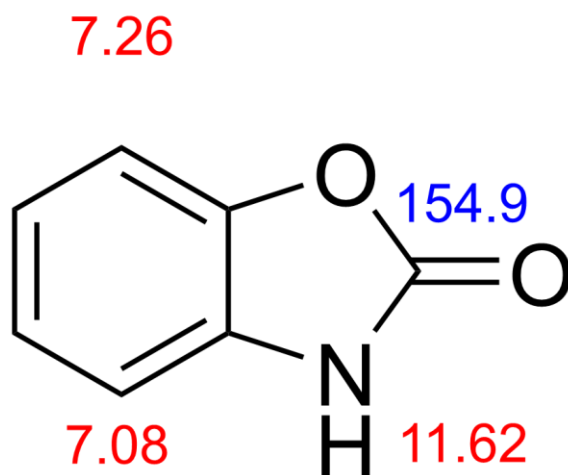


Figure 21. Partial NMR assignment of compound 1 following NOESY and COSY analysis. Carbon assignments are in blue. Proton assignments are in red.

$^1\text{H}$ - $^{13}\text{C}$  HSQC was analyzed next. A list of the observed interactions can be found in the table below, as well as images of the spectra.

Table 7. List of observed HSQC interactions. The individual signals' chemical shifts as well as multiplicities were discerned using this two dimensional spectrum.

Carbon atom (ppm)	Hydrogen atom (ppm) and multiplicity
123.8	7.13 triplet
121.8	7.07 triplet
109.8	7.08 doublet
109.5	7.26 doublet
154.4	None
143.3	None
130.3	None

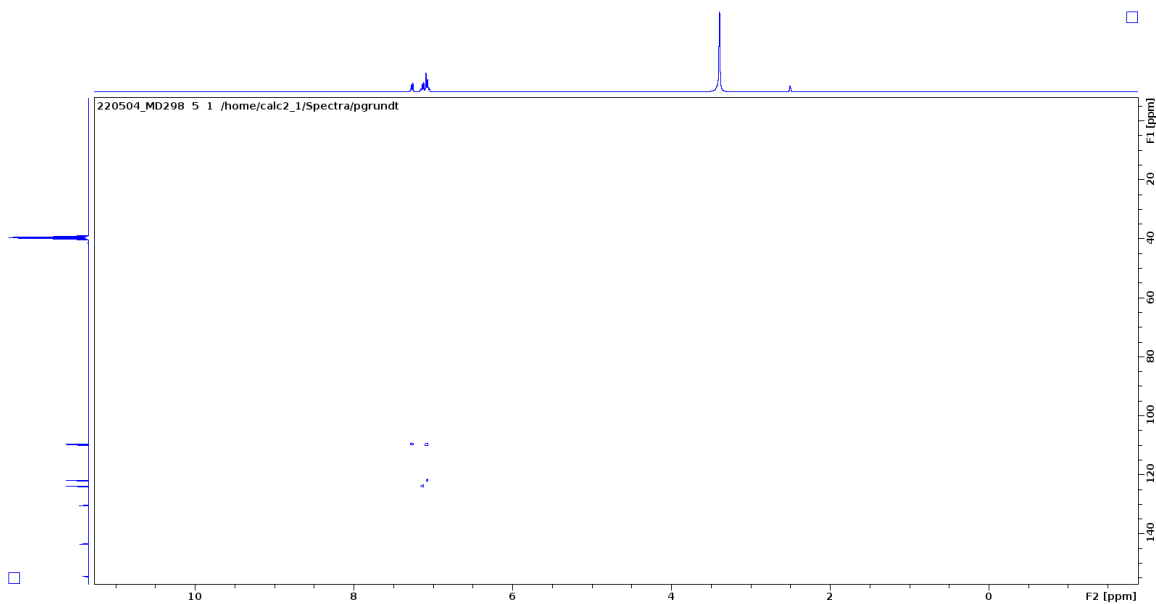


Figure 22. Full HSQC spectrum for compound 1.

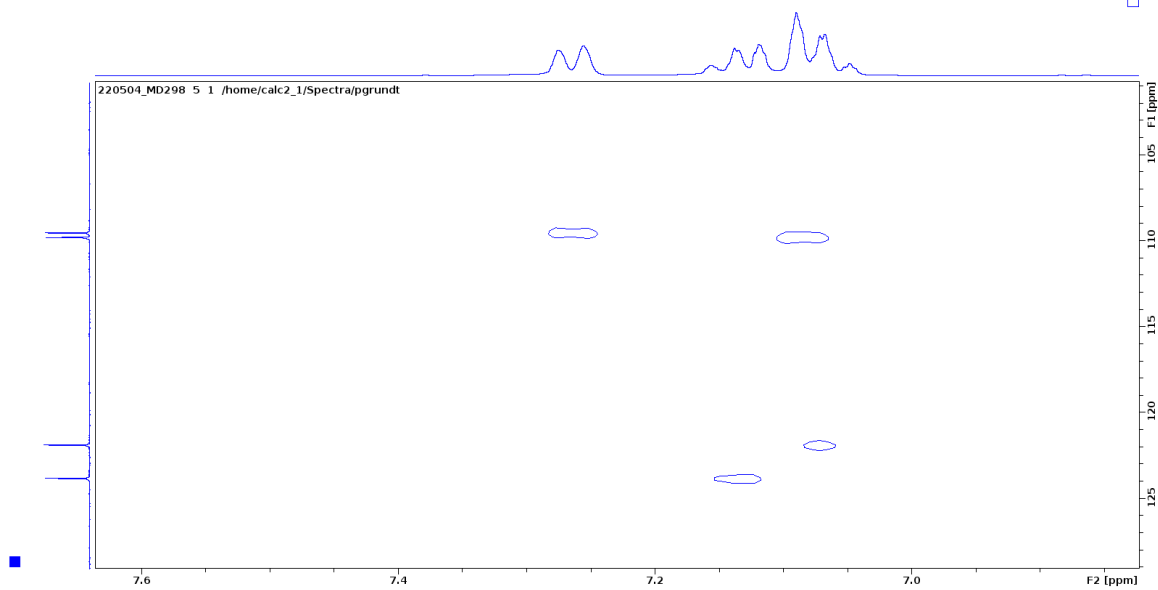


Figure 23. Aromatic region of HSQC for compound 1.

HSQC spectra show interactions between hydrogens and carbons that are 1 bond away; in other words, they show which hydrogens are attached to specific carbons. This helps us make a couple of assignments at this time, and it will be useful later. The updated assignments can be seen below.

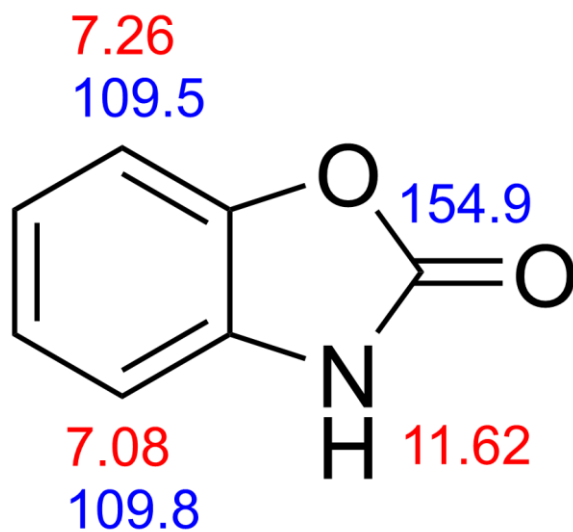


Figure 24. Partial assignment for compound 1 following HSQC analysis. Carbon assignments are in blue. Proton assignments are in red.

The next NMR technique used was  $^1\text{H}$ - $^{13}\text{C}$  HMBC, which visualizes interactions between hydrogens and carbons that are three bonds away. This ultimately allowed us to assign the rest of the structure. Images of the spectra can be found below.

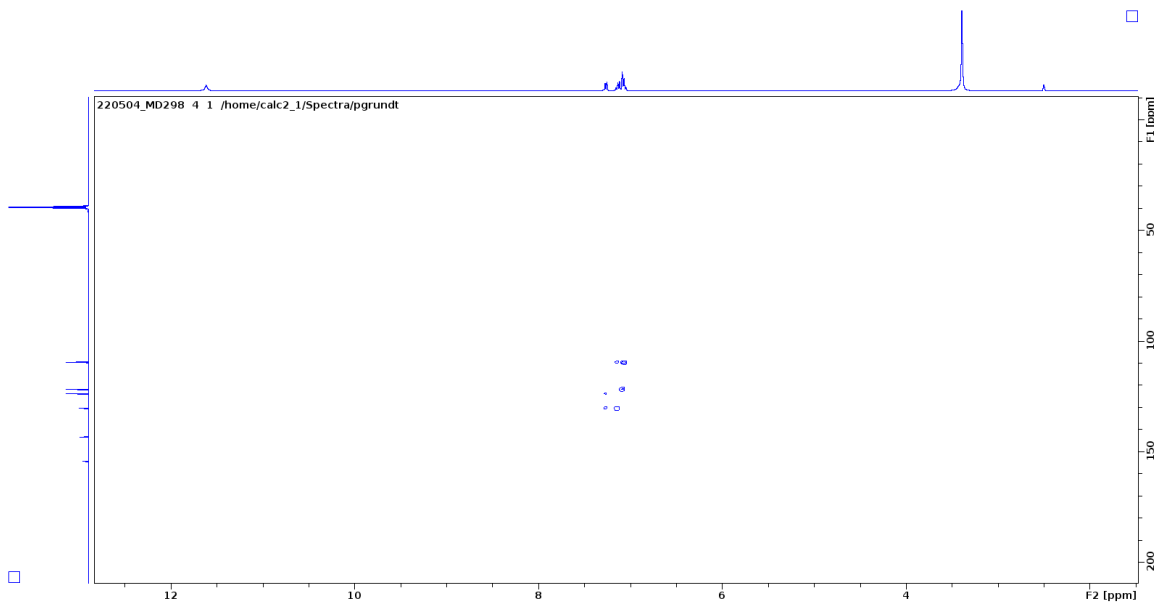


Figure 25. Full HMBC Spectrum for compound 1.

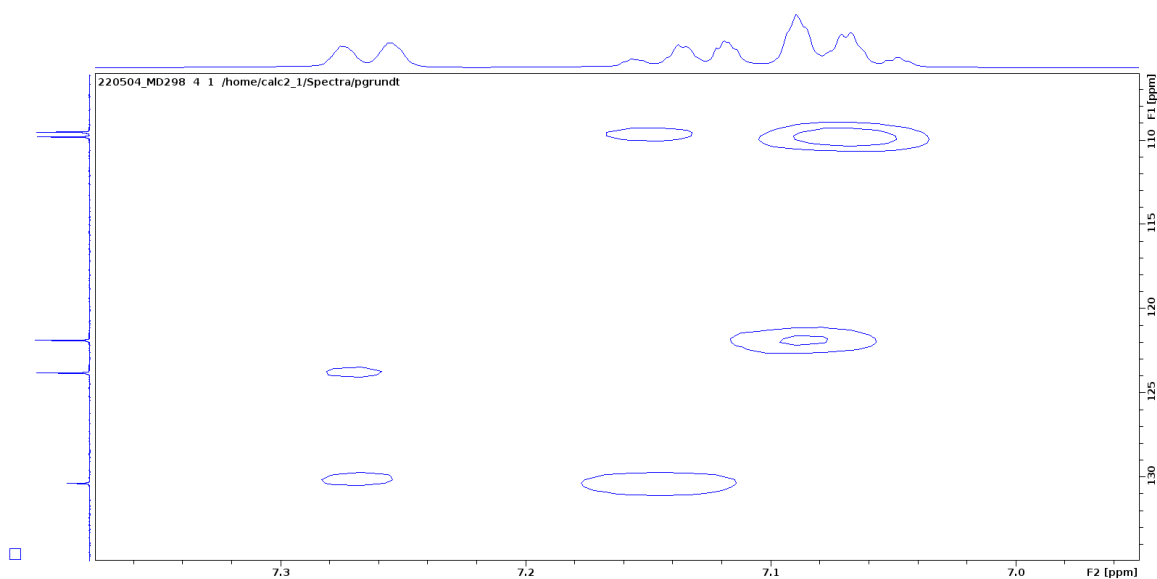


Figure 26. Aromatic Region of HMBC Spectrum for compound 1.

Initially, the signals belonging to the N-H proton were looked at. We expected to see an interaction between that proton and the 7a position carbon as well as the 4-position carbon. Unfortunately, no such signals appeared. This is why the 7.26 ppm doublet needed to be assigned earlier through COSY, otherwise we would not have access to the aromatic ring.

A table of the important interactions can be seen below.

Table 8. List of the most intense interactions in the HMBC.

Proton Atom (ppm)	Carbon atom(s) (ppm)
7.26	130.3
	123.7
7.13	109.5
	130.3

7.08	121.8
7.07	109.8
11.62	None

By following through with the above interactions, the following assignments were made. The interaction between 7.26 ppm and 123.7 ppm suggests that carbon belongs in the 5 position, and its proton can be assigned through the previous HSQC spectrum. Similarly, the interaction between the 7.08 ppm and 121.8 ppm signals suggests that carbon belongs in the 6 position, and its proton can be assigned through HSQC. The only carbon assignments left at this point are the 4a and 7a carbons. A 130.3 ppm carbon signal can be seen by the protons with chemical shifts of 7.26 ppm and 7.13 ppm. That strongly suggests that assignment belongs in the 4a position, which leaves the 143.3 ppm to be assigned in the 7a position. At this point all shifts have been assigned and can be visualized below.

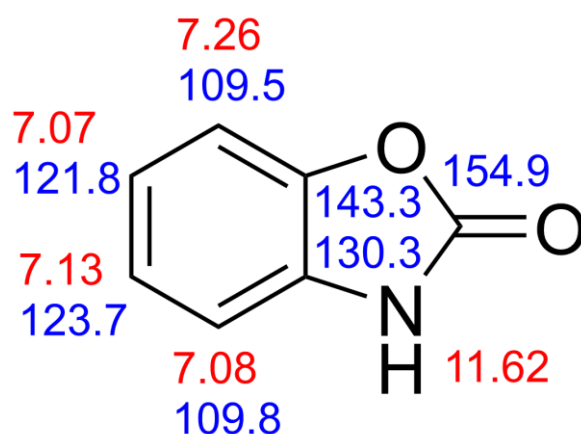


Figure 27. Full Assignment of compound 1. Carbon assignments are in blue. Proton assignments are in red.

The remaining analysis will make sure that no disagreements lie with the rest of the spectral data. Returning to the HMBC, the 7.07 ppm triplet signal has an interaction with 109.8 ppm, which agrees with our assignment. We are expecting an interaction with the 143.3 ppm carbon as well, however that cannot be seen in our spectrum, even with the floor lowered to allow for lower intensity signals. The 7.08 ppm doublet signal has an interaction with the 121.8 ppm carbon, which is in agreement with our assignment, however we are also expecting an interaction with the 143.3 ppm carbon, which again is not seen in our spectrum. At this point, the 143.3 ppm signal was assigned solely because it was the last one left, and it proves to be elusive in these spectra. In an attempt to try and find some evidence for its assignment the floor was lowered in the HMBC to see lower intensity signals. Generally speaking, this makes analysis more difficult because 2 and 4 bond interactions become more prevalent, and at similar intensities, making it difficult to decide which to go with. Fortunately, we have made our assignments already so this should be an issue.

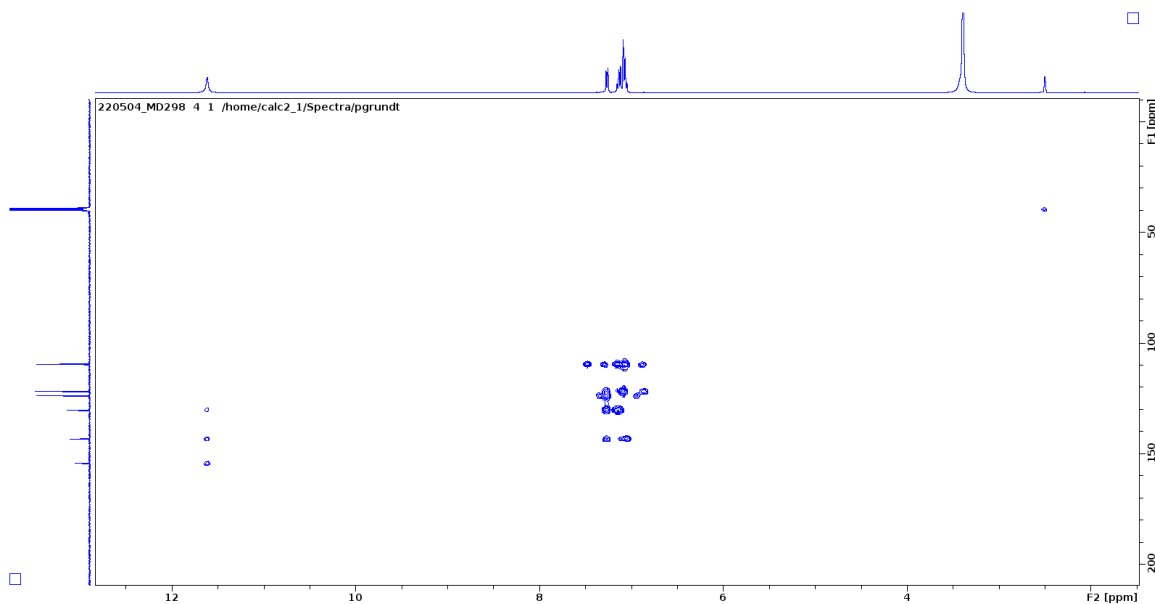


Figure 28. Full HMBC Spectrum with raised floor to see weaker interactions.



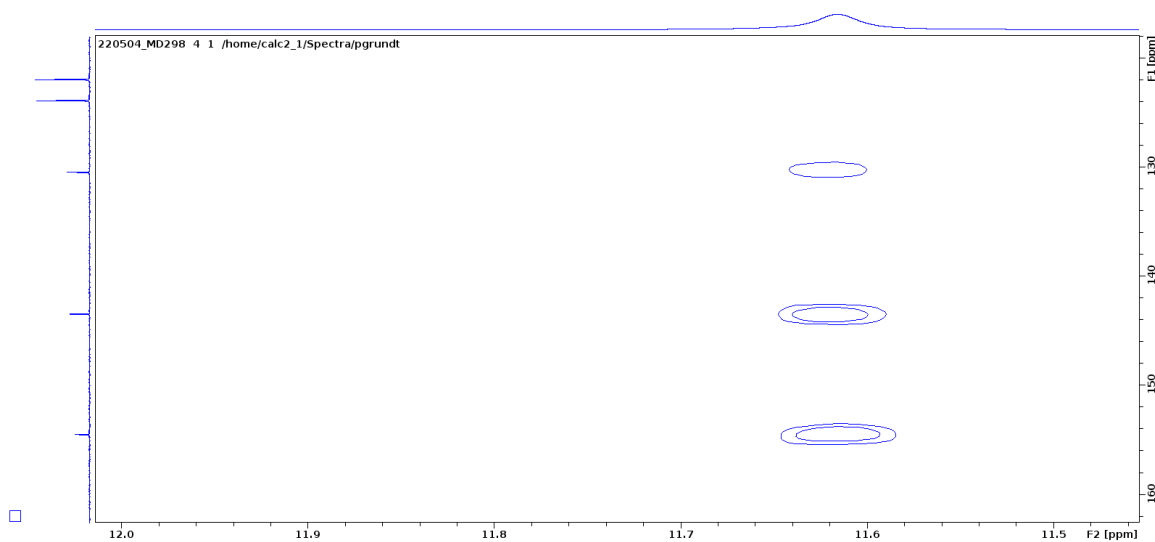


Figure 29. Full HMBC Spectrum with raised floor to see weaker interactions. The signals belonging to the N-H proton are focused.

Overall, the 2 and 4 bond interactions in the aromatic region are less useful to deducing structure, however what is seen from the 11.62 ppm N-H signal is important. Three signals can be seen here. First, a 2 bond interaction can be seen with the 154.9 ppm amide carbon, as expected. The next signal is a 3 bond interaction with the elusive 143.3 ppm carbon. The third signal, which is a slightly lower intensity than the other two signals, is an interaction with the 130.3 ppm carbon, which is 2 bonds away.

Finally, an  $^1\text{H}$ - $^{15}\text{N}$  HMBC was measured. As can be seen below, only a 1 bond interaction between the nitrogen and the N-H proton was observed. It was hoped that we could visualize the interaction between the 7.08 ppm proton and the nitrogen to make for a more sound initial assignment, but that cannot be seen in the spectrum.

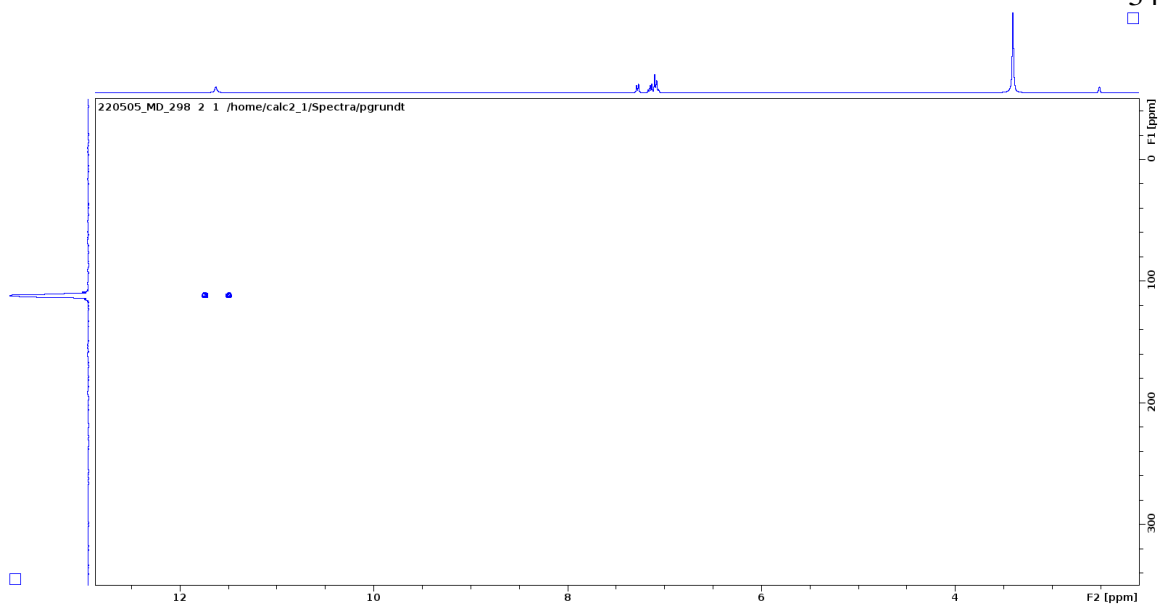


Figure 30. Full  $^1\text{H}$ - $^{15}\text{N}$  HMBC Spectrum for compound 1.

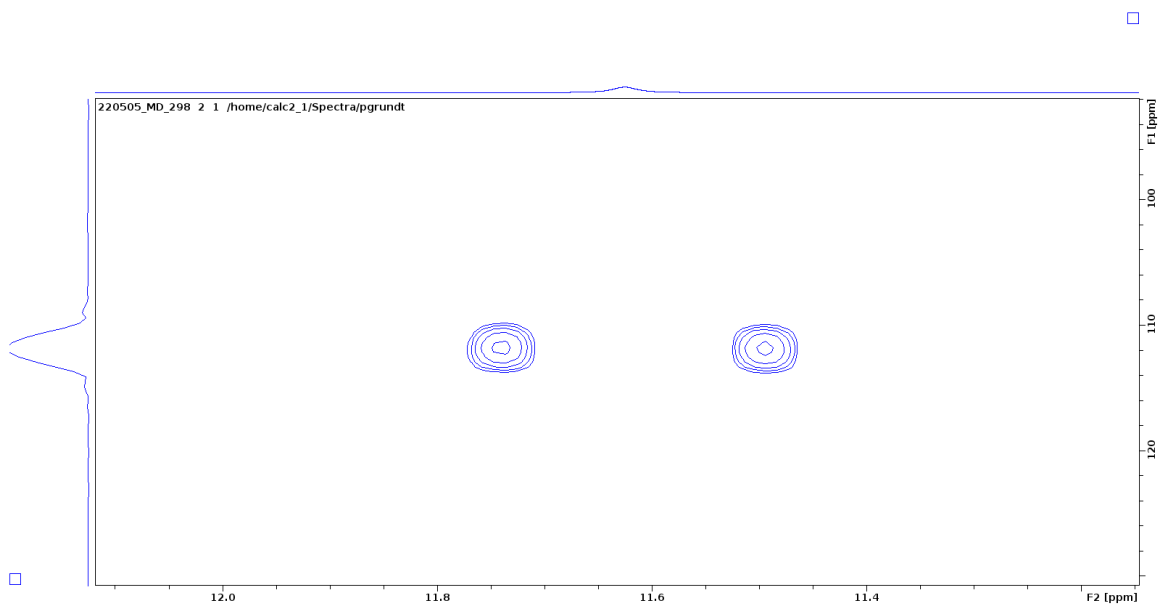


Figure 31.  $^1\text{H}$ - $^{15}\text{N}$  HMBC Spectrum focused on the only available signal.

This concludes the NMR characterization of this compound. Many other NMR experiments were performed in an attempt to more clearly see some of these signals, such as the 7.08 vs. 7.26 assignment or the 143.3 ppm signal by changing the NMR acquisition settings, such as looking for different coupling constants, but it has proved difficult with our current equipment. Still, the assignment above has little to no disagreements with our data, so we can make a confident characterization here.

### Compound 2

A proton and carbon NMR were measured for this compound. The spectra can be seen below.

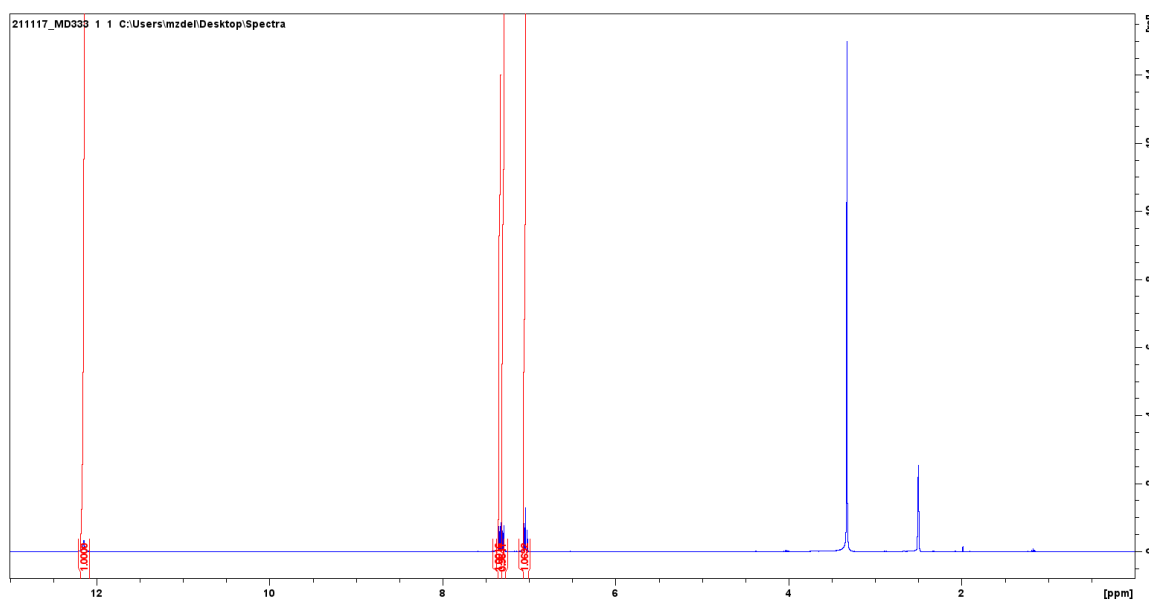


Figure 32. Full  $^1\text{H}$  NMR Spectrum for compound 2.

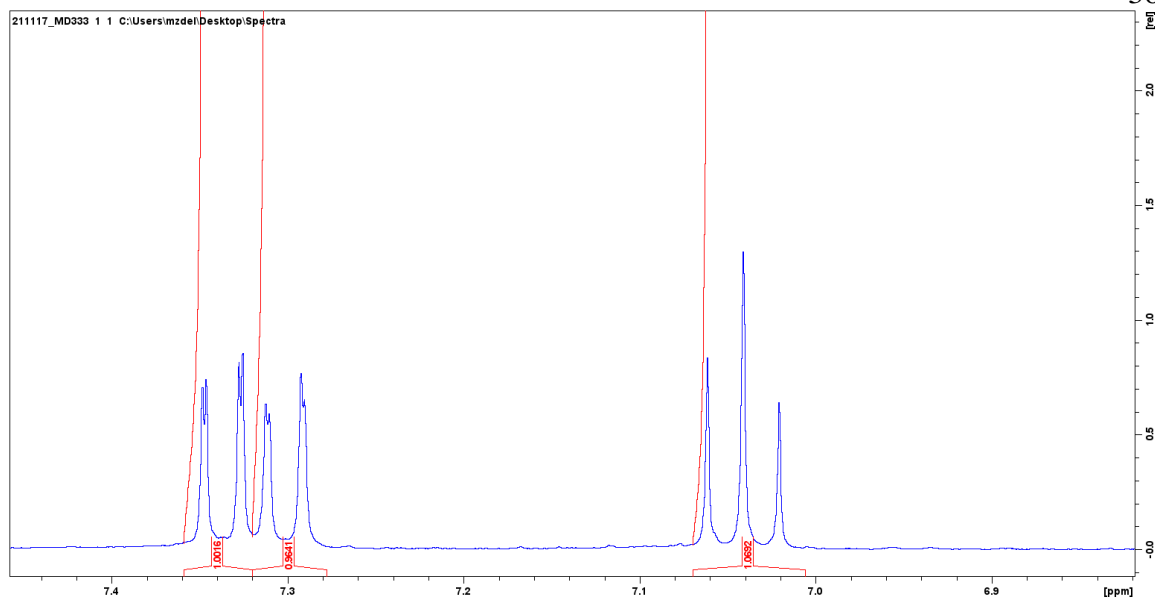


Figure 33. Aromatic region of  $^1\text{H}$  NMR spectrum.

One of the signals are highly shifted at 12.15 ppm, which is what we expect for the N-H signal. The rest of the signals fall in the aromatic region, with all of them integrating to three, which is expected for this compound. A clear triplet signal can be seen with a coupling constant of 8.1 Hz, most likely arising from the 3 bond coupling between the nearby hydrogens. This suggests this signal belongs to the hydrogen in position 6. Next are the two doublet of doublet signals, which have coupling constants of 8.1 Hz and 0.9 Hz, which arise from 3 bond and 4 bond coupling, respectively. These belong to hydrogens in the 5 and 7 positions, however we cannot discern which one is which based on this information alone. Overall, the  $^1\text{H}$  NMR spectrum lines up with what we expect for this compound.

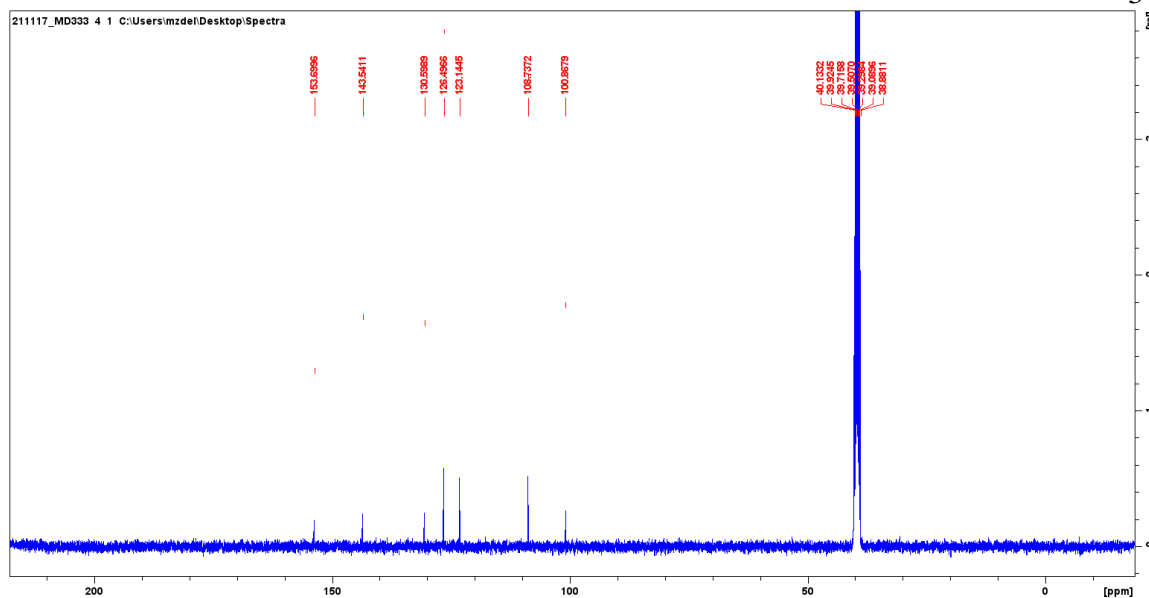


Figure 34. Full  $^{13}\text{C}$  NMR Spectrum for compound 2.

The carbon NMR gives us seven total signals, which is what we expect for this molecule. One signal, the highest shifted one at 153.7 ppm matches what we would expect for the carbonyl carbon. The rest of the signals belong to the aromatic ring and match what we would expect for these derivatives.

### Compound 3

A  $^1\text{H}$  and  $^{13}\text{C}$  spectrum were acquired for this compound, which can be seen below.

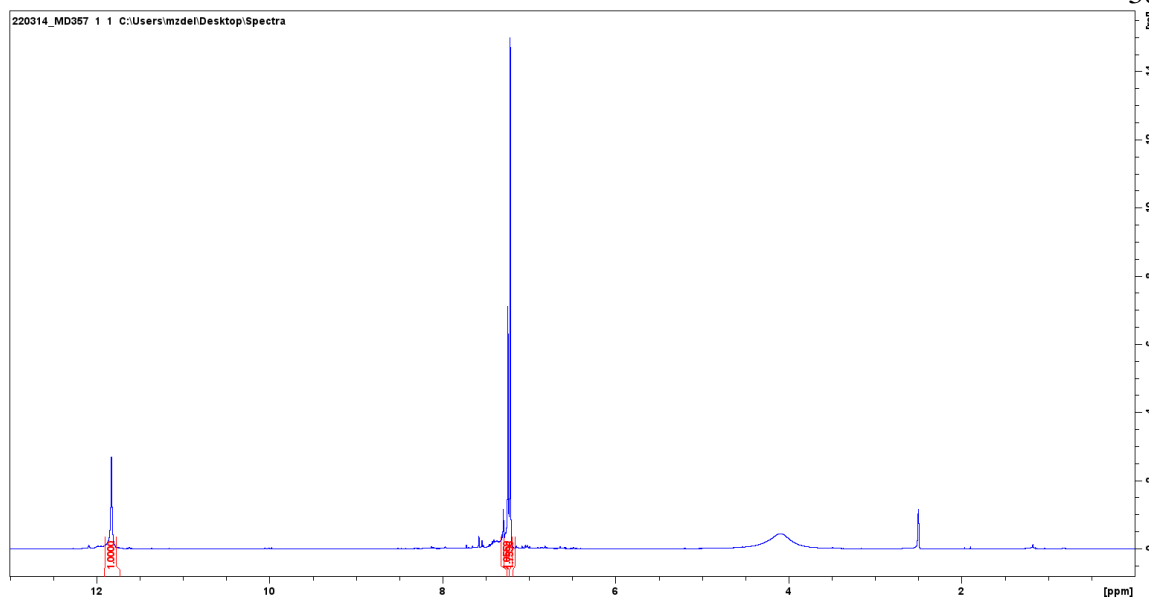


Figure 35. Full  $^1\text{H}$  Spectrum for compound 3. Peak around 4 ppm is due to water.

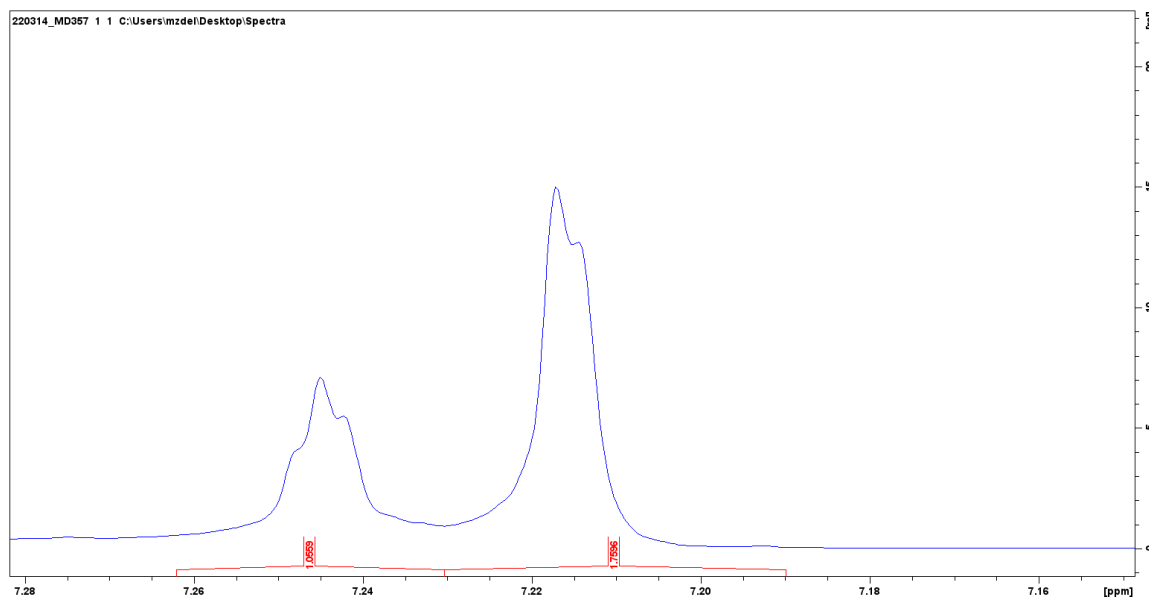


Figure 36. Aromatic region of  $^1\text{H}$  Spectrum for compound 3.

The  $^1\text{H}$  signals together integrate to four, which is what is expected for this molecule.

One highly shifted signal at 11.83 ppm belongs to the N-H proton, while the other three

signals lie in the aromatic region. We would expect two doublets and a singlet for this molecule if we are just taking into account normal 3 bond coupling. Here, two of the aromatic signals overlapped forming a multiplet, while the other nearby signal appears to be a triplet, which is not expected for this molecule. The most likely cause of this is that the 7.25 ppm signal is due to a doublet of doublets with a small coupling constant, so that the two doublets are still overlapping. Then the 2H would be composed of a singlet and a doublet with a small coupling constant corresponding to a 4 bond coupling. This would roughly match the shape we see here and the type of coupling patterns we see in other derivatives. However, to know for sure some higher resolution spectra would have to be acquired.

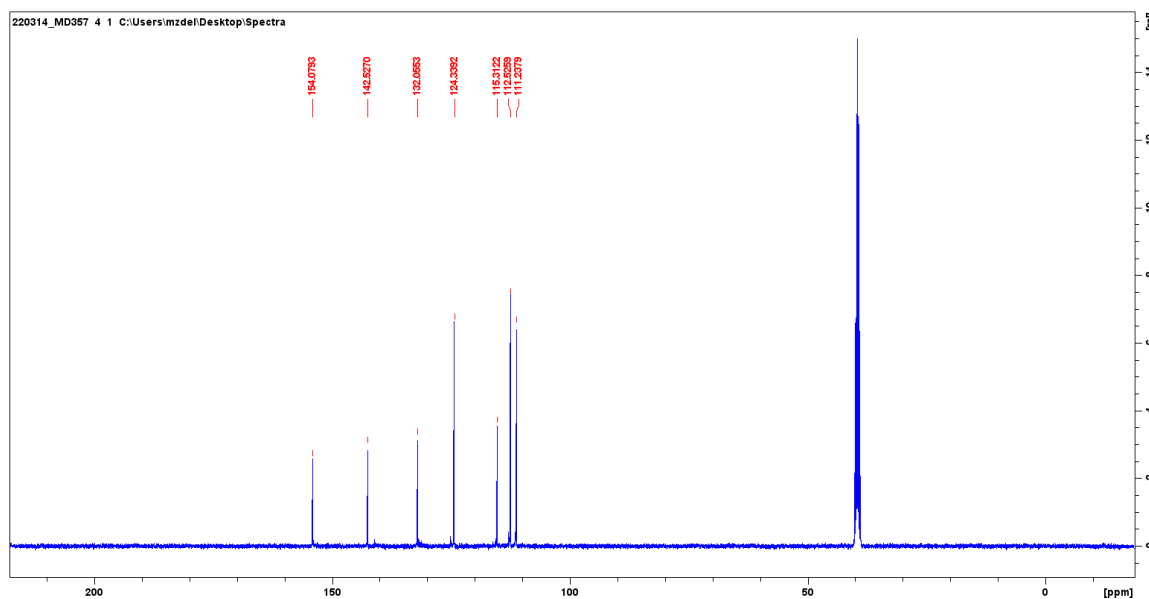


Figure 37. Full  $^{13}\text{C}$  Spectrum for compound 3.

The  $^{13}\text{C}$  spectrum gives seven total signals which is in line with this molecule. All of the signals follow the expected behavior for these derivatives. The highest shifted carbon is

at 154.1 ppm, which falls in line with the carbonyl carbon in these compounds. The rest of the signals belong to the aromatic ring.

### Compound 4

A  $^1\text{H}$  and  $^{13}\text{C}$  spectrum were acquired for this compound, which can be seen below.

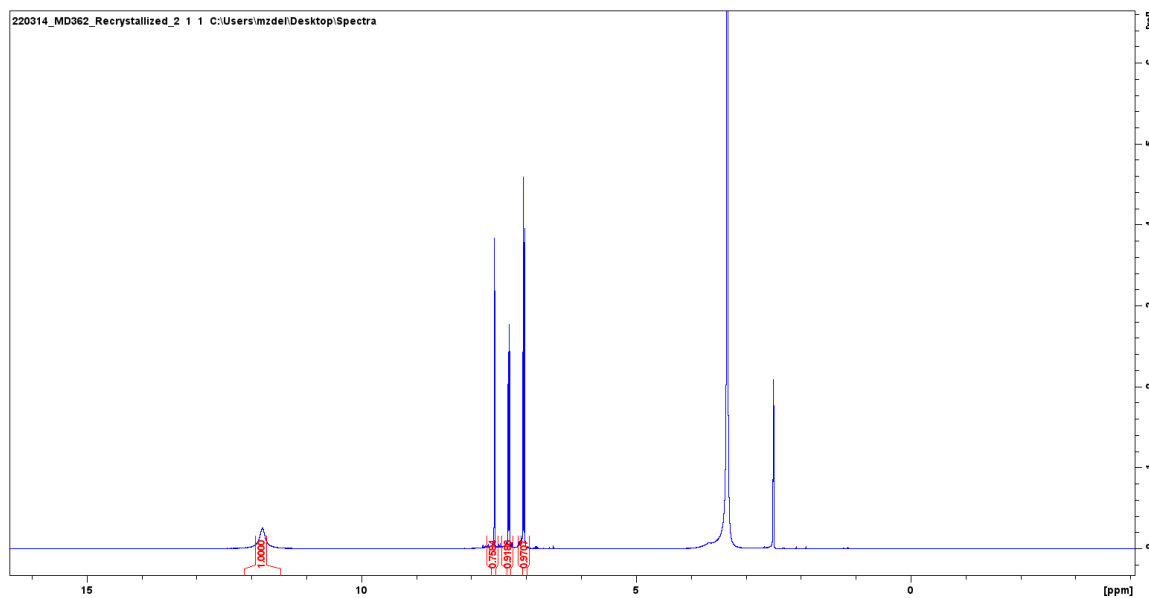


Figure 38. Full  $^1\text{H}$  Spectrum for compound 4. Signal at 3.34 ppm is due to water.



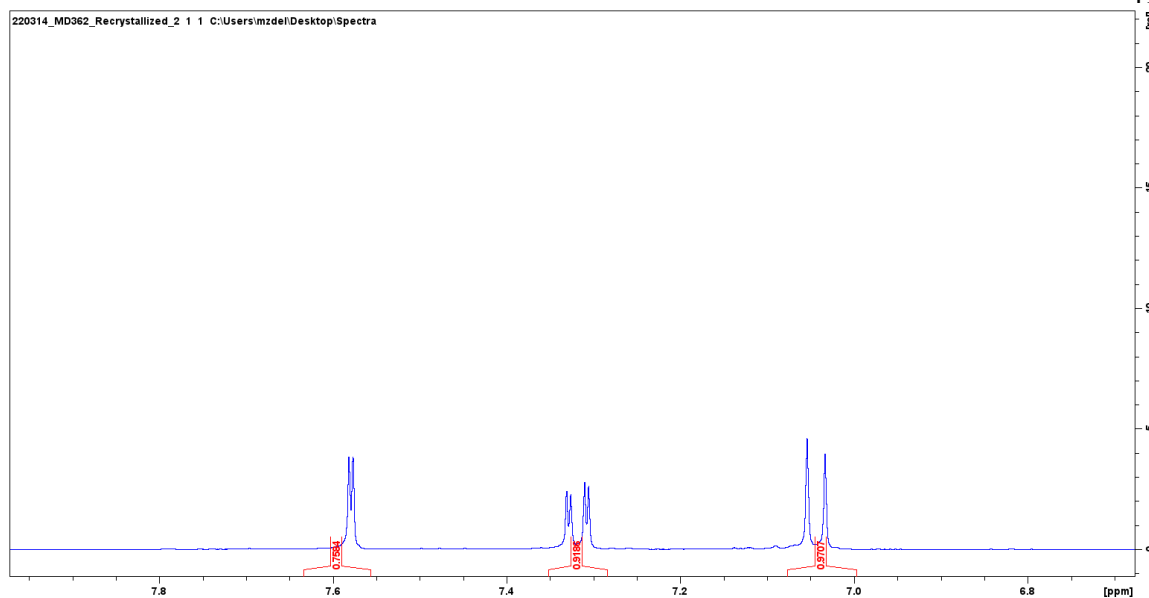


Figure 39. Aromatic region of  $^1\text{H}$  Spectrum for compound 4.

All of the  $^1\text{H}$  signals integrate to 4H, which is what is expected for this molecule. The highest shifted signal at 11.80 ppm belongs to the N-H peak, while the other three belong to the aromatic protons. Focusing in on the aromatic region we can see three well defined signals. First, the signal at 7.58 ppm is a doublet with a small coupling constant, corresponding to 1.9 Hz, which matches four bond proton coupling. This signal belongs to the proton in position 7. Next, there is a signal at 7.32 ppm which is a doublet of doublets. This experiences the 4 bond coupling as well as the 3 bond coupling (8.3 Hz) to the nearby hydrogens, so this belongs to position 5. Finally the last signal at 7.05 ppm experiences only three bond coupling, so it belongs to position 4.

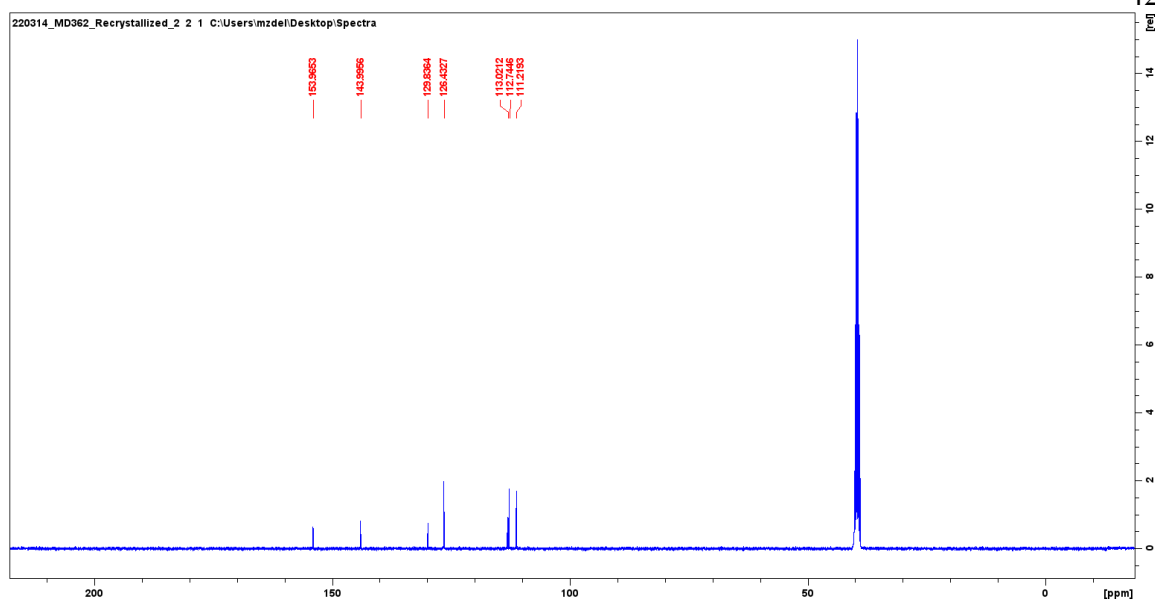


Figure 40. Full  $^{13}\text{C}$  Spectrum for compound 4.

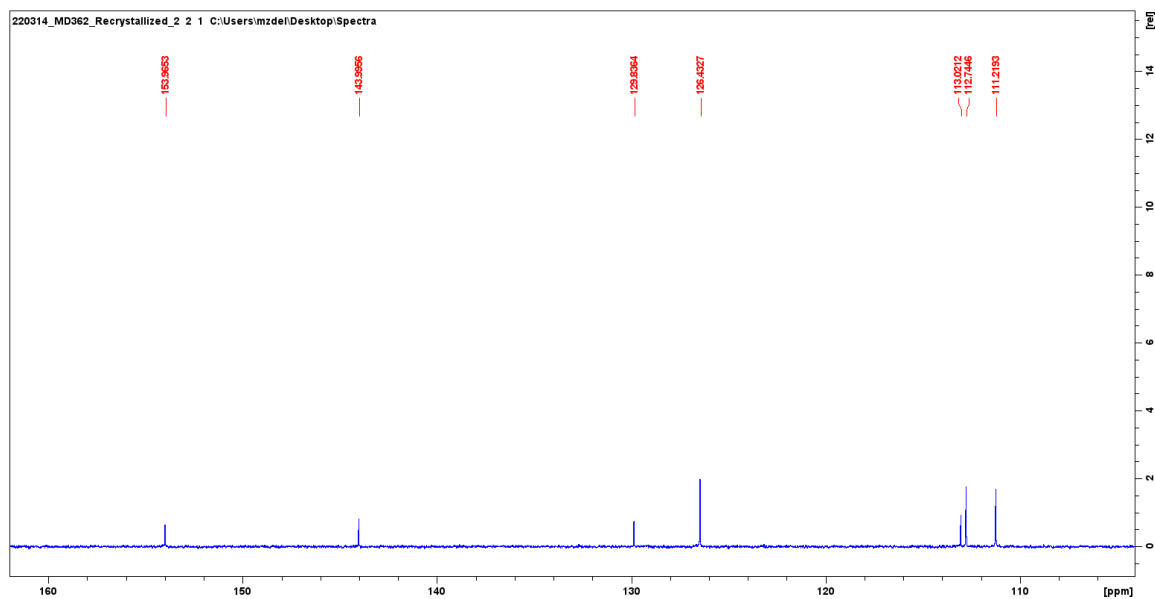


Figure 41. Zoomed in  $^{13}\text{C}$  Spectrum for compound 4. The signals can now be distinguished between 110 and 115 ppm.

A total of 7 signals are given in this  $^{13}\text{C}$  spectrum, which matches what is expected for this compound. The highest shifted carbon, at 154.0 ppm belongs to the carbonyl, and matches what is expected for this compound. The rest of the signals belong to the aromatic ring.

### Compound 5

A  $^1\text{H}$  and  $^{13}\text{C}$  spectrum were acquired for this compound, which can be seen below.

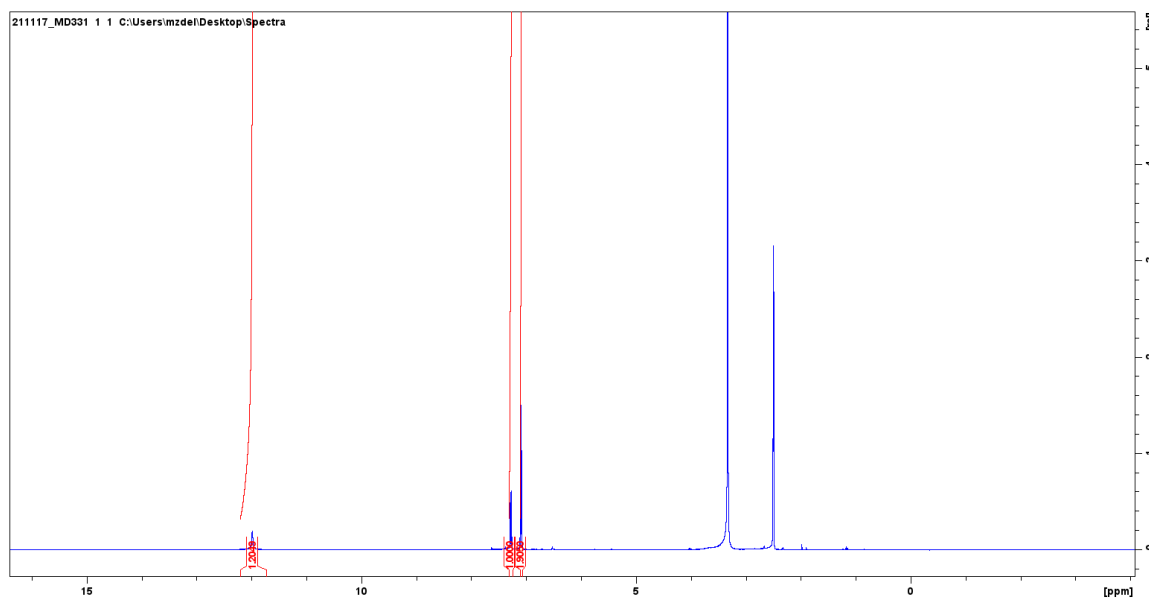


Figure 42. Full  $^1\text{H}$  Spectrum for compound 5. Peak at 3.34 ppm is due to water.

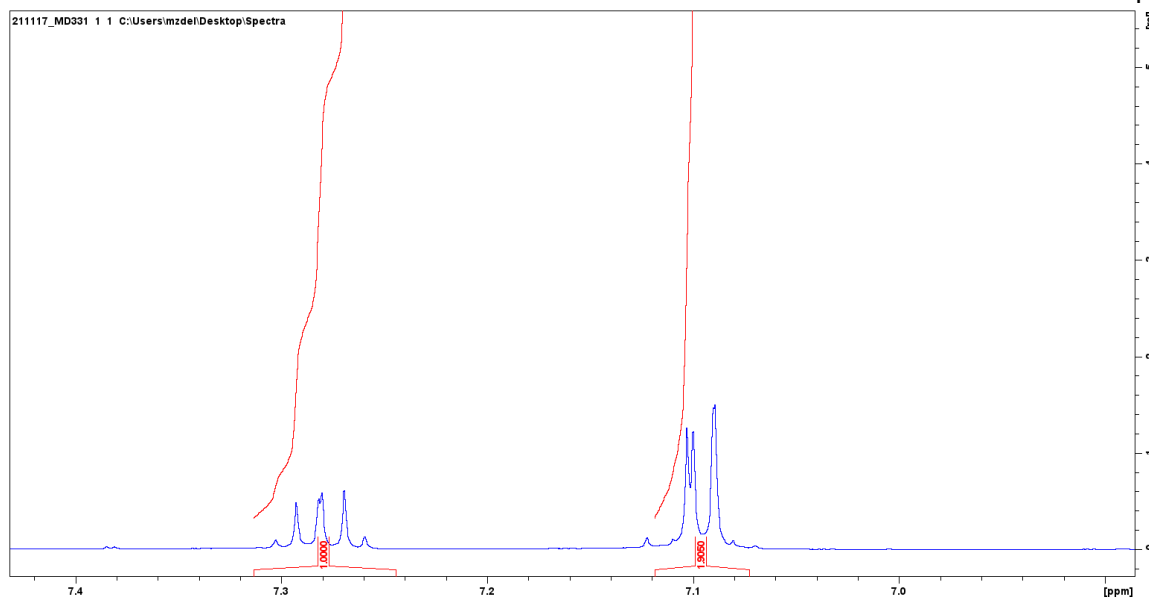


Figure 43. Aromatic region of  $^1\text{H}$  Spectrum for compound 5.

All of the proton signals integrate to four, which is expected for this compound. The highest shifted signal at 11.99 ppm corresponds to the N-H proton, while the rest belong to the aromatic ring. The rest of the signals lie in the aromatic region and integrate to 3H, which is what we would expect for this derivative. The first signal is a multiplet from 7.25-7.31 ppm. The remainder signals are a doublet at 7.10 ppm ( $J = 1.2$  Hz), and a singlet at 7.09 ppm. This leaves us with an unexpected aromatic splitting pattern; for this molecule we would expect two doublets and a triplet. This behavior is most likely due to higher order coupling, and is outside the scope of this work.

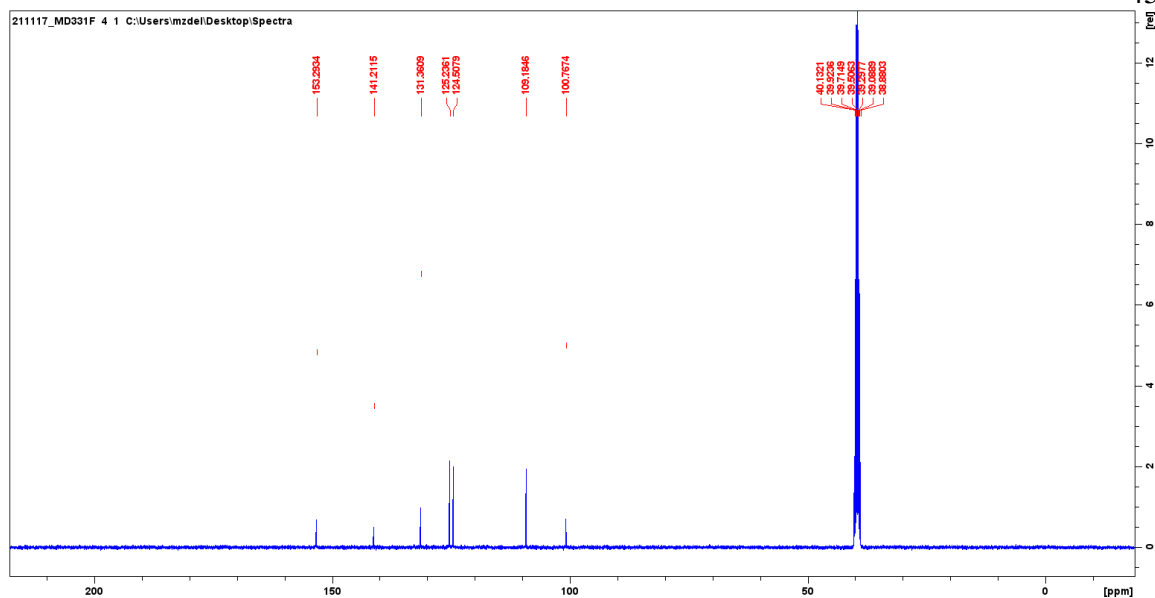


Figure 44. Full  $^{13}\text{C}$  Spectrum for compound 5.

The  $^{13}\text{C}$  spectrum gave seven total signals which is expected for this molecule. The highest shifted signal at 153.3 ppm belongs to the carbonyl, which is similar to the other derivatives. The remainder of the signals belong to the aromatic ring.

### Compound 6

A  $^1\text{H}$  and  $^{13}\text{C}$  spectrum were acquired for this compound, which can be seen below.

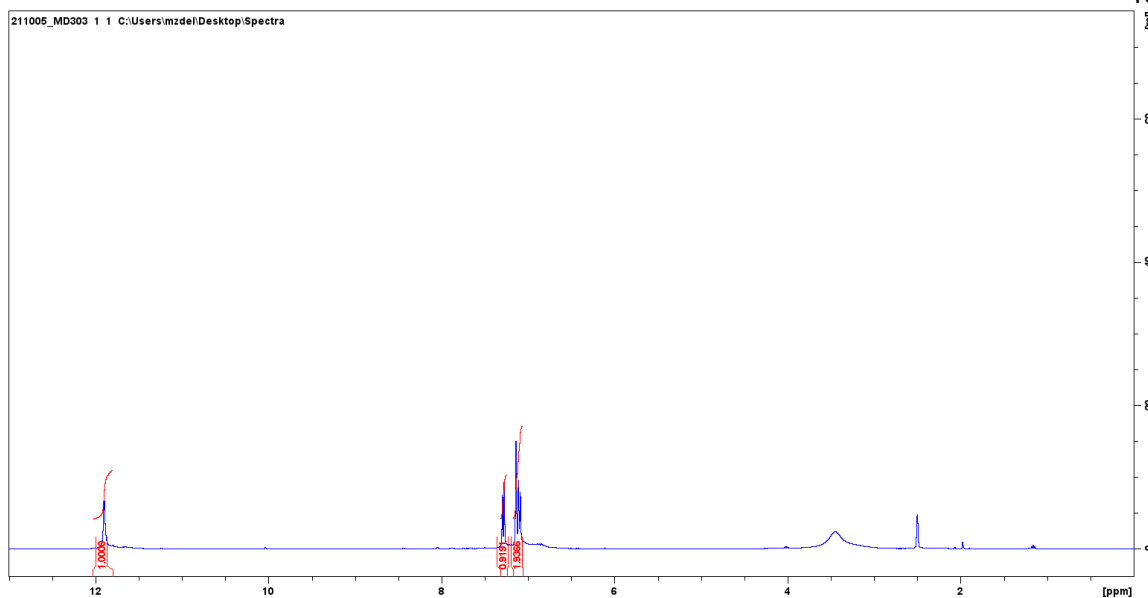


Figure 45. Full  $^1\text{H}$  Spectrum for compound 6. Peak at 3.45 is due to water.

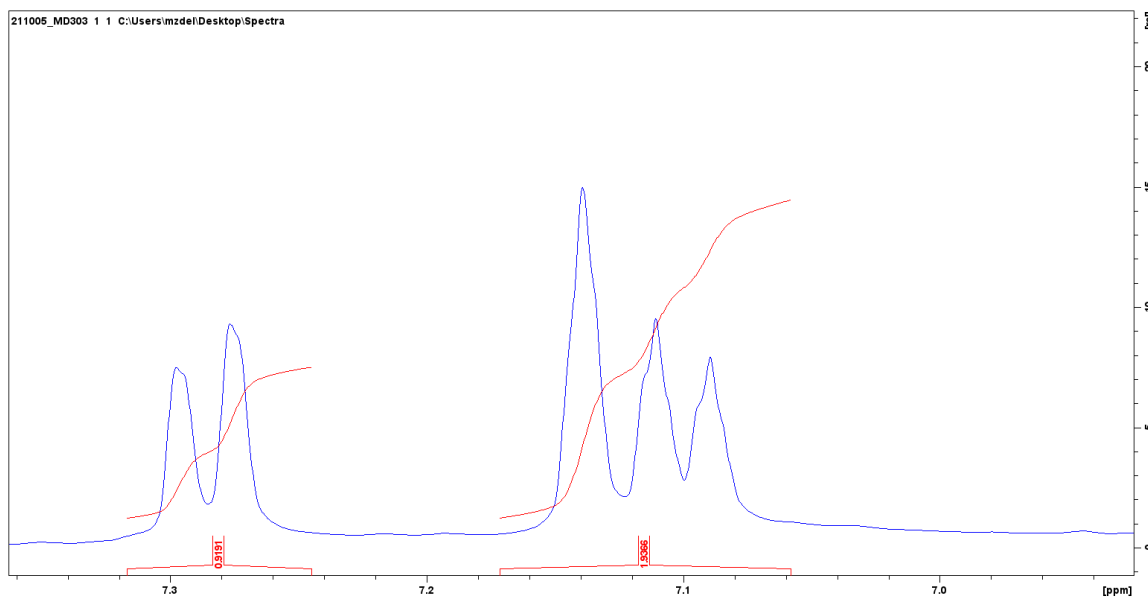


Figure 46. Aromatic region of  $^1\text{H}$  Spectrum for compound 6.

All of the proton signals integrate to 4H, which is expected for this compound. The highest shifted signal at 11.90 ppm belongs to the N-H proton, while the rest belong to

the aromatic ring. The first aromatic signal is a doublet at 7.29 ppm with a coupling constant of 8.5 Hz. The next signal is a singlet at 7.14 ppm, and then the last signal is a doublet at 7.10 ppm with a coupling constant of 8.5 Hz. These two signals are very close to each other, but the signals were separated by recognizing the coupling constant in the doublet on the right. Overall, this makes sense given the substitution pattern in the aromatic ring.

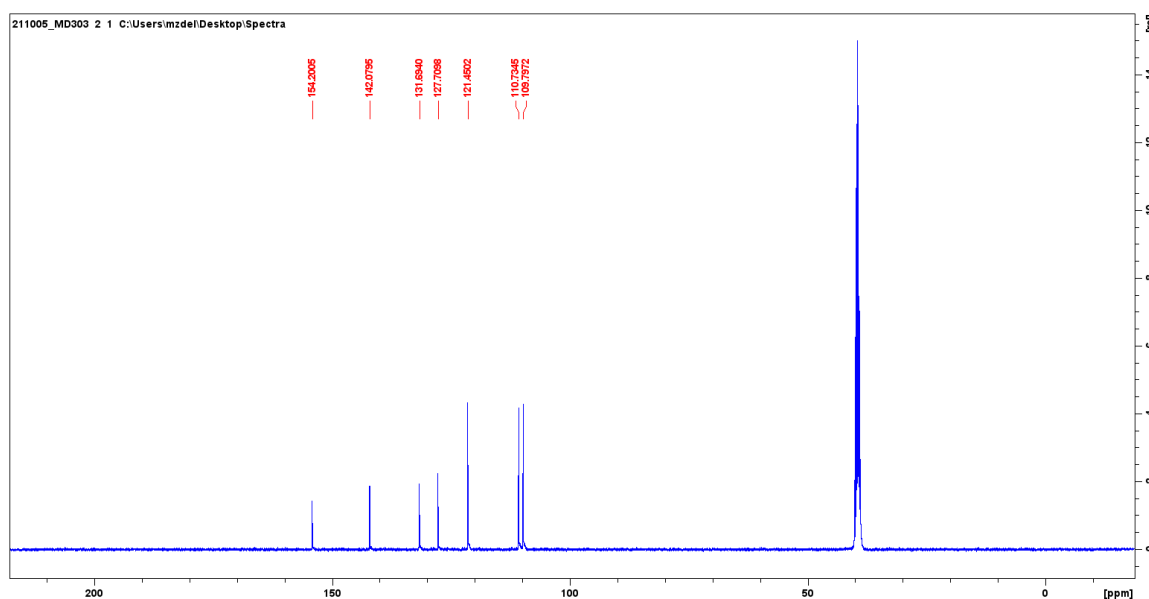


Figure 47. Full  $^{13}\text{C}$  Spectrum for compound 6.

The  $^{13}\text{C}$  spectrum gave a total of seven signals which is expected for this compound. The highest shifted signal lies at 154.2 ppm, which is similar to other derivatives. The remainder of the signals belong to the aromatic ring and their shifts all fall in line with what we have seen with the other derivatives.

Compound 7

A  $^1\text{H}$  and  $^{13}\text{C}$  spectrum were acquired for this compound, which can be seen below.

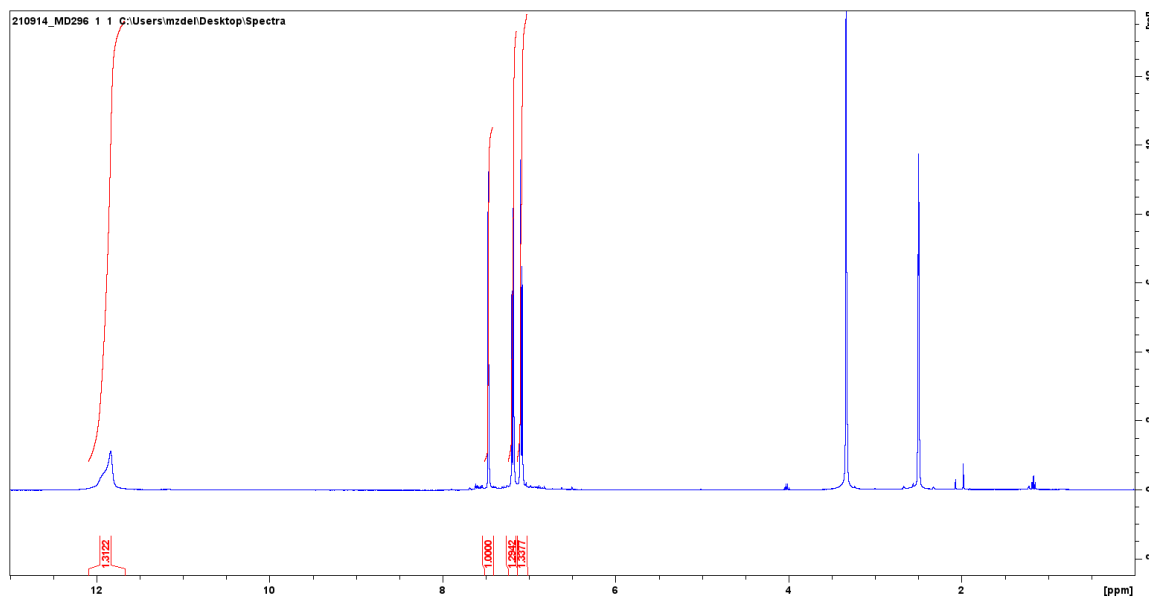


Figure 48. Full  $^1\text{H}$  Spectrum for compound 7. Peak at 3.33 is due to water.

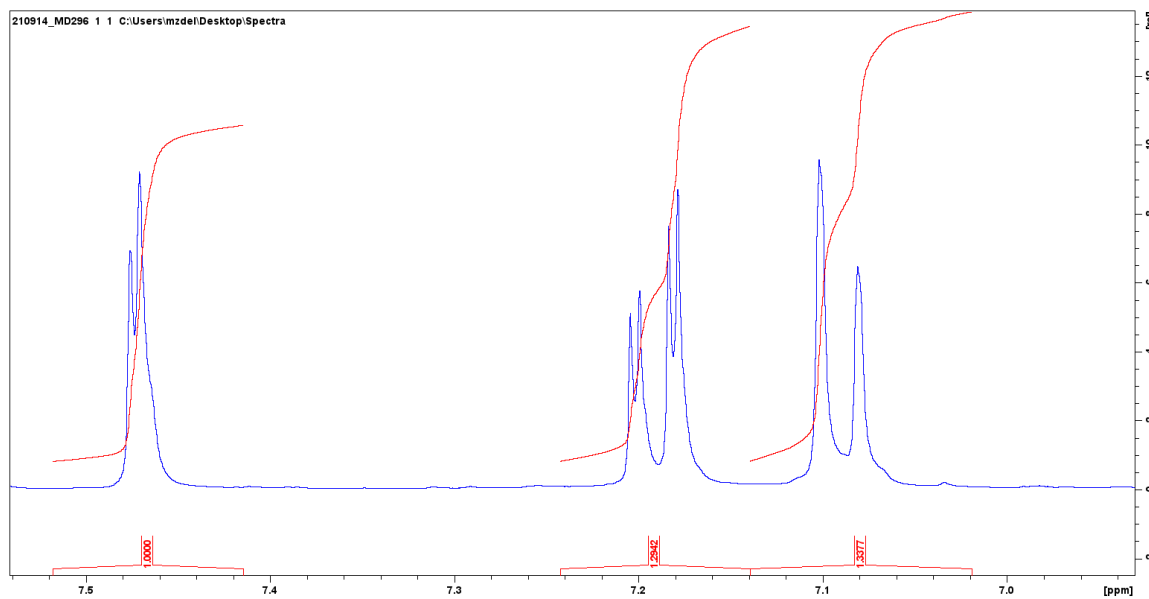


Figure 49. Aromatic Region of  $^1\text{H}$  Spectrum for compound 7.



All of the proton signals integrate to 4H, which is expected for this compound. The highest shifted signal at 11.84 ppm belongs to the N-H proton, while the rest belong to the aromatic ring. The first aromatic signal is a doublet at 7.47 ppm with a coupling constant of 2.0 Hz. This likely corresponds to 4 bond coupling, so this signal belongs to the proton in the 7 position. The next signal is a doublet of doublets at 7.19 ppm with the coupling constants 8.3 and 2.0 Hz. This means this proton has a 3 and 4 bond coupling with nearby hydrogens, which would make sense for the proton in position 5. The last signal is a doublet at 7.09 ppm with a coupling constant of 8.3 Hz. This proton has a 3 bond coupling with the neighboring hydrogen, which makes sense for the 4 position.

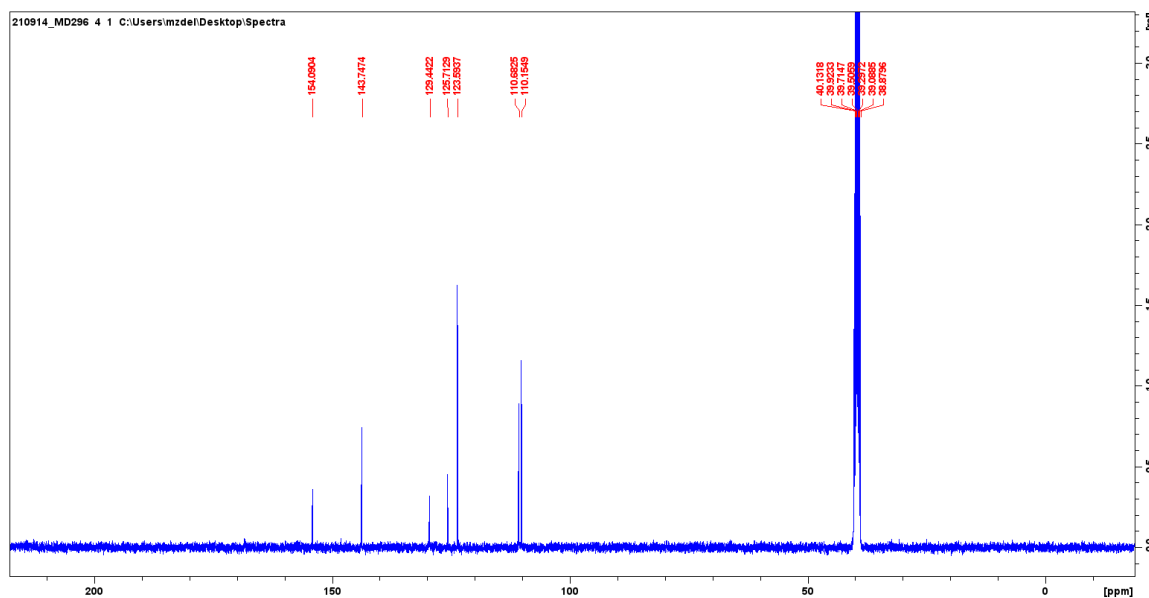


Figure 50. Full  $^{13}\text{C}$  Spectrum for compound 7.

The  $^{13}\text{C}$  spectrum gave a total of seven signals which is expected for this compound. The highest shifted signal lies at 154.1 ppm, which is similar to other derivatives. The

remainder of the signals belong to the aromatic ring and their shifts all fall in line with what we have seen with the other derivatives.

### Compound 8

A  $^1\text{H}$  and  $^{13}\text{C}$  spectrum were acquired for this compound, which can be seen below.

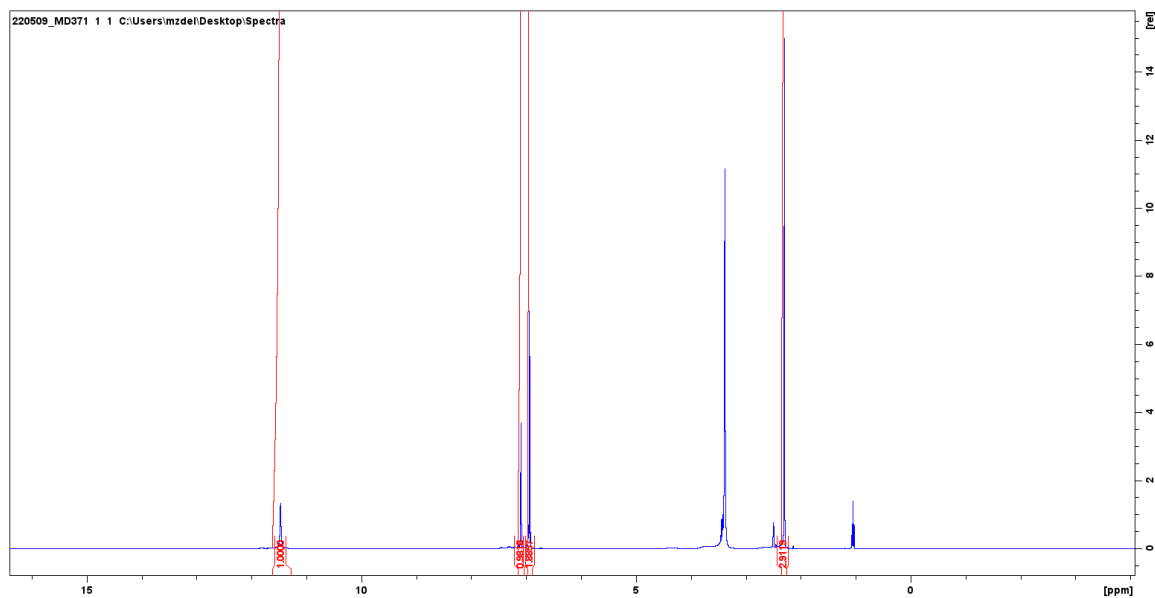


Figure 51. Full  $^1\text{H}$  Spectrum for compound 8. Peak at 3.38 is due to water.

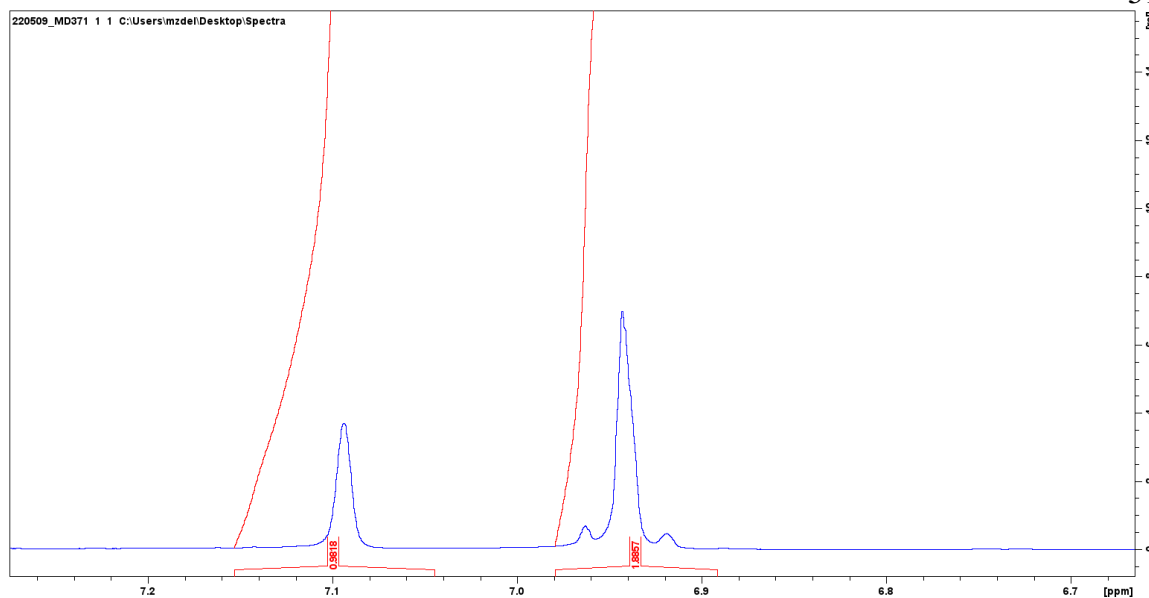


Figure 52. Aromatic region of  $^1\text{H}$  Spectrum for compound 8.

All of the protons integrate to 7H in this molecule, which makes sense given its structure. The highest shifted peak at 11.47 ppm belongs to the N-H proton and matches what we would expect for these derivatives. In the alkyl region we can observe a 3H singlet signal that belongs to the methyl group at 2.30 ppm. In the aromatic region we have one singlet at 7.09 ppm, and then a 2H multiplet at 6.91-6.97 ppm. We would expect a singlet and two doublets in the aromatic region, so it is entirely possible that two doublets overlapped to form the multiplet signal.

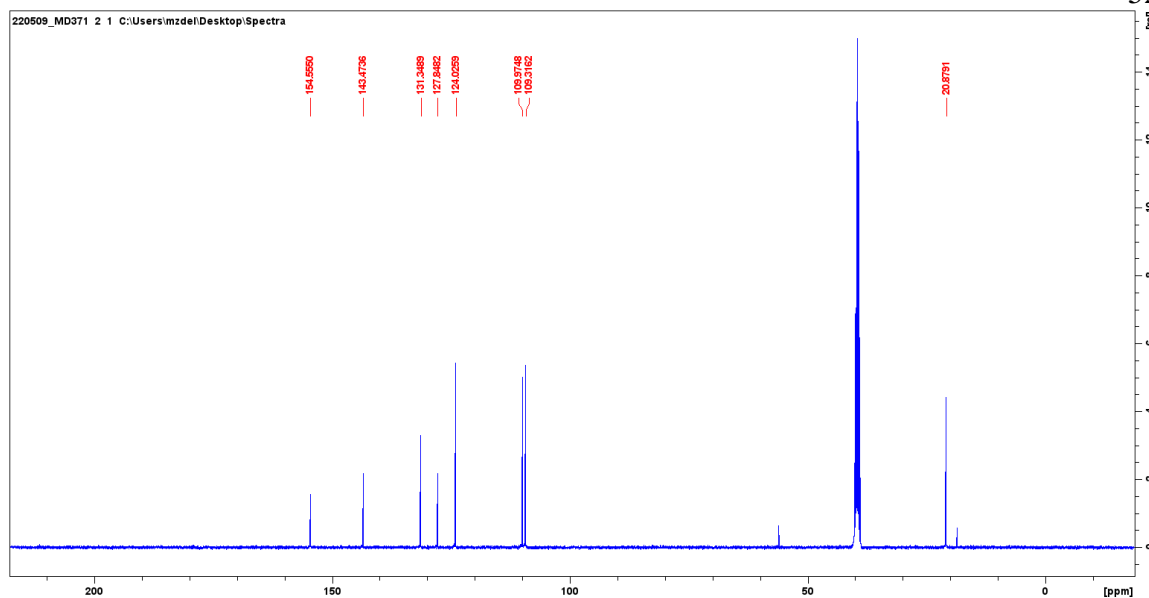


Figure 53. Full  $^{13}\text{C}$  Spectrum for compound 8. The signals at 56.1 and 18.5 ppm are due to methanol.

The  $^{13}\text{C}$  spectrum gives a total of 8 signals, which is to be expected for this compound. The highest shifted signal lies at 154.6 ppm, which belongs to the carbonyl and matches what we see in other derivatives. The signal at 20.9 ppm belongs to the methyl group, which matches what is expected for alkyl groups. The remainder of the signals belong to the aromatic ring, and their behavior is similar to what we see in other derivatives.

### Compound 9

A  $^1\text{H}$  and  $^{13}\text{C}$  spectrum were acquired for this compound, which can be seen below.

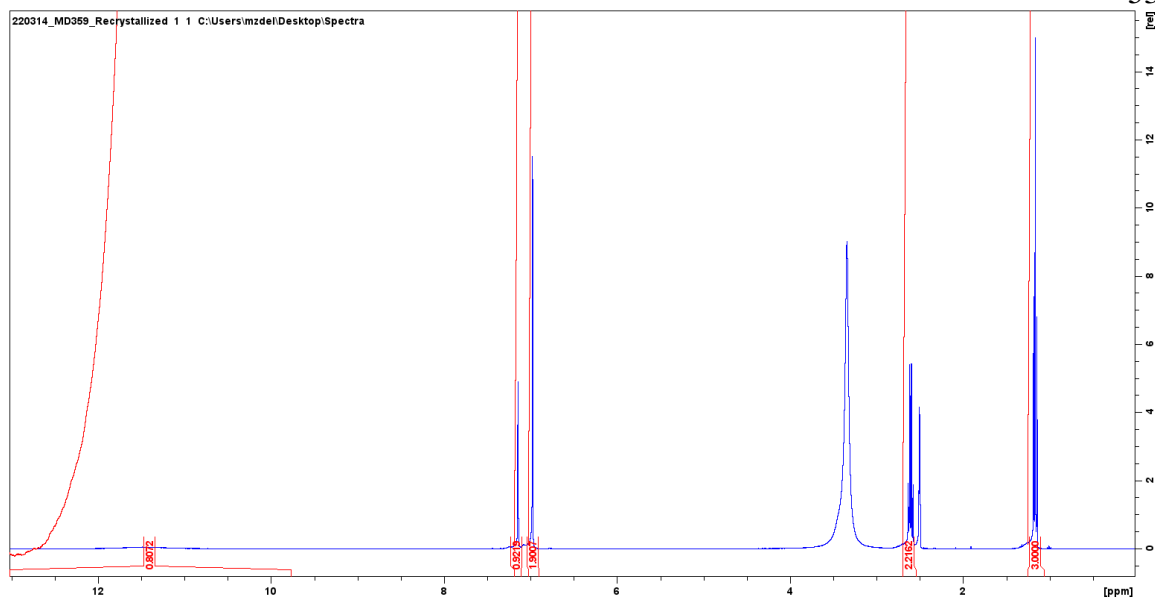


Figure 54. Full  $^1\text{H}$  Spectrum for compound 9. Peak at 3.34 is due to water.

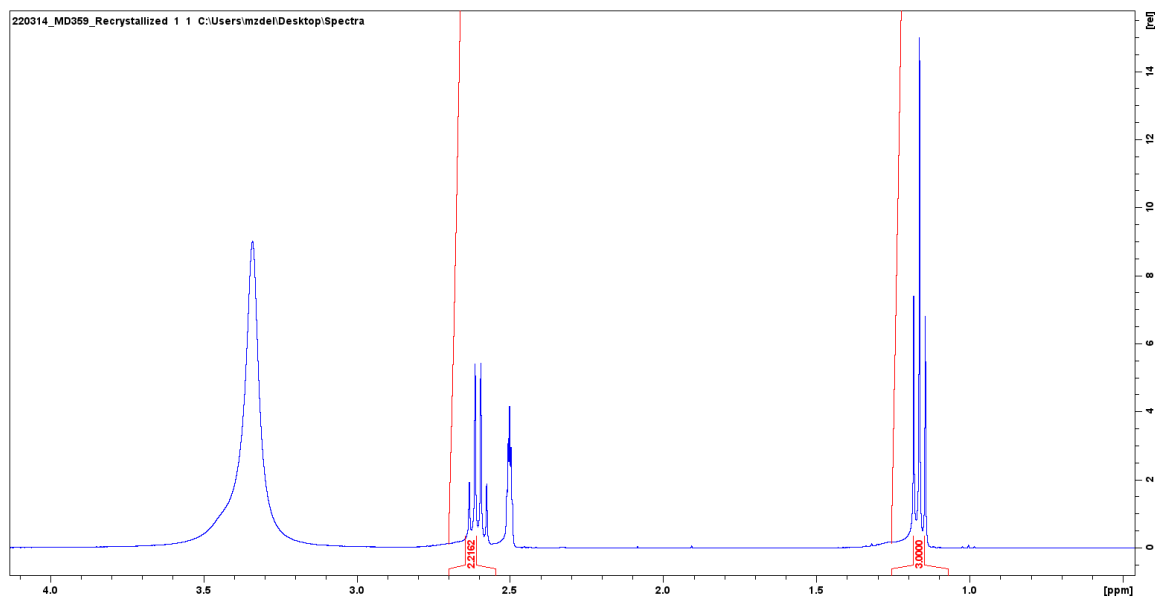


Figure 55. Alkyl region of  $^1\text{H}$  Spectrum for compound 9. Peak at 3.34 is due to water and peak at 2.50 is due to DMSO.

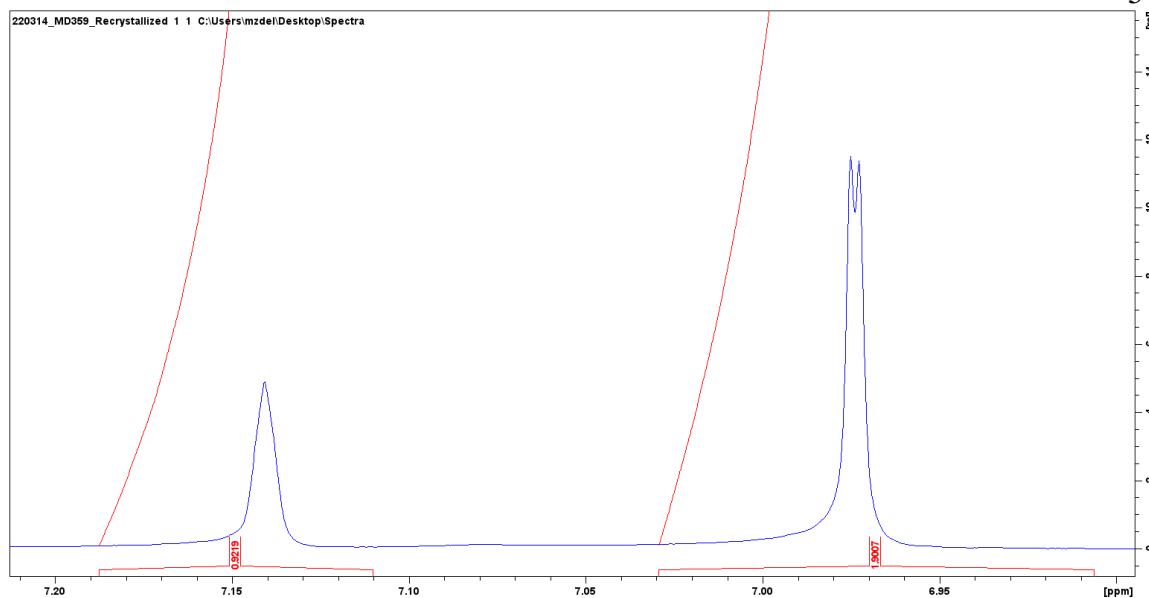


Figure 56. Aromatic region of  $^1\text{H}$  Spectrum for compound 9.

All of the protons integrate to 9H in this molecule, which makes sense given its structure. The highest shifted peak at 11.47 ppm belongs to the N-H proton and matches what we would expect for these derivatives. In the alkyl region we can observe a 2H quartet at 2.60 ppm with a coupling constant of 7.6 Hz, suggesting three bond coupling. A 3H triplet at 1.16 ppm with a coupling constant of 7.5 Hz can also be observed. This matches what would be expected for an alkyl group in the molecule. In the aromatic region we are expected two doublets and a singlet. At 7.14 ppm we can observe a 1H singlet, and at 6.97 ppm there is a 2H multiplet. Similar to the 6-methyl derivative, it seems that these two doublets may have overlapped to form this multiplet.

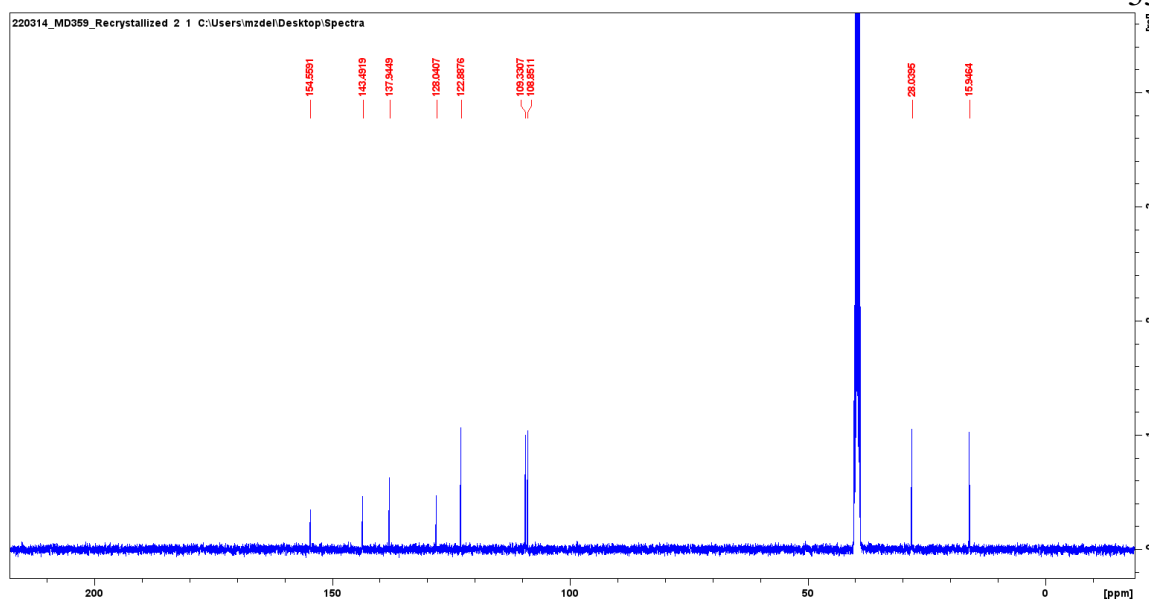


Figure 57. Full  $^{13}\text{C}$  Spectrum for compound 9.

The  $^{13}\text{C}$  spectrum gives a total of 9 signals, which is to be expected for this compound. The highest shifted signal lies at 154.6 ppm, which belongs to the carbonyl and matches what we see in other derivatives. The signal at 28.0 and 15.9 ppm belongs to the ethyl group. The remainder of the signals belong to the aromatic ring, and their behavior is similar to what we see in other derivatives.

### Compound 10

A  $^1\text{H}$  and  $^{13}\text{C}$  spectrum were acquired for this compound, which can be seen below.

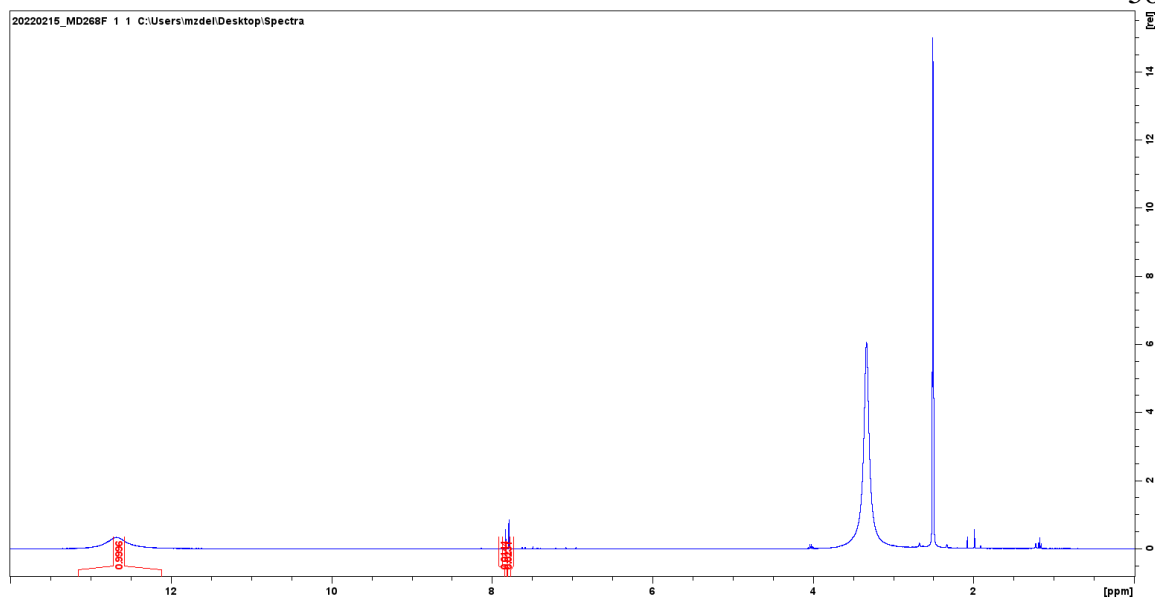


Figure 58. Full  $^1\text{H}$  Spectrum for compound 10. Peak at 3.33 is due to water.

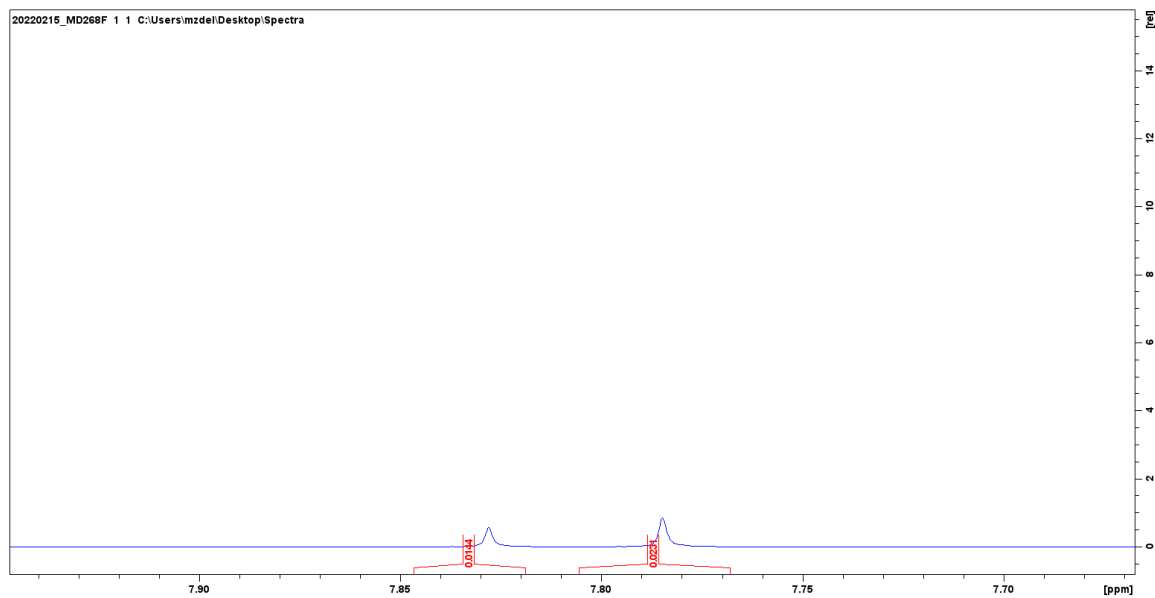


Figure 59. Aromatic region of  $^1\text{H}$  Spectrum for compound 10.



Since this derivative's aromatic ring is saturated with bromines, this spectrum looks a bit different. The only major signal is at 12.68 ppm. This likely belongs to the N-H proton and is a little higher shifted than most of the other derivatives; for comparison, the unsubstituted compound shifts at 11.62 ppm. This is to be expected through for a derivative with many electronegative atoms; in general, electron withdrawing groups tend to increase the chemical shifts in a molecule. Other than that, there are no major signals in the proton NMR, which follows what we would expect for this molecule. It is worth noting there are minor signals (integrating to 0.01) in the aromatic region. These likely belong to other compounds that did not fully convert to the tetrabromine compound. Their identity will be discussed later. These could not be removed through recrystallization or chromatography with the instruments we had available.

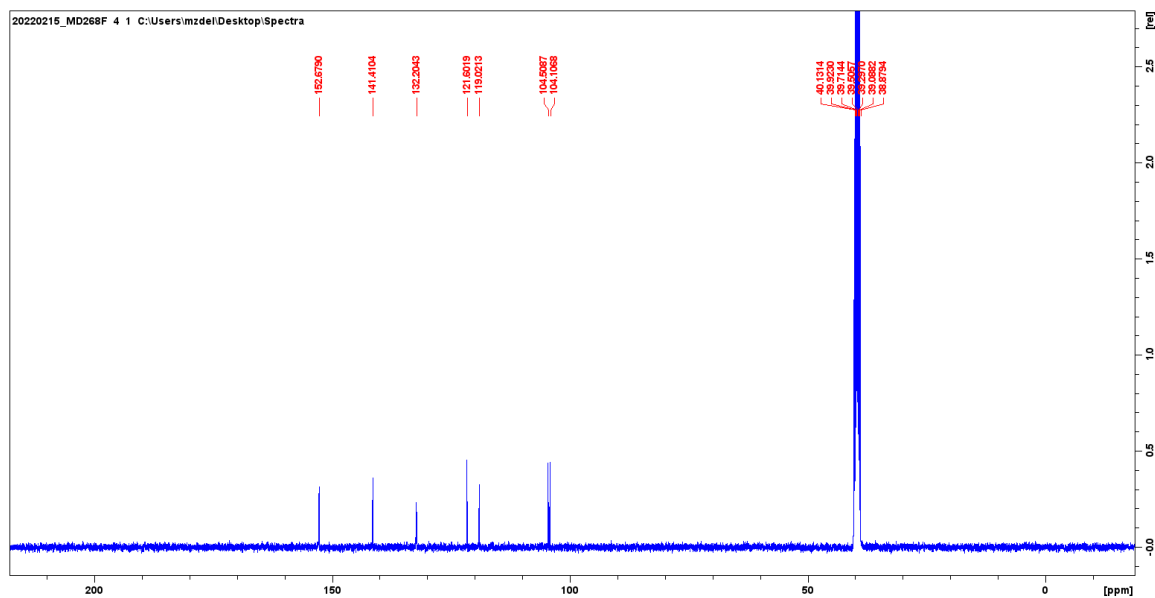


Figure 60. Full  $^{13}\text{C}$  Spectrum for compound 10.

The  $^{13}\text{C}$  spectrum gives a total of seven signals, which is what we would expect for this compound. The highest shifted signal is at 152.7 ppm, which is about what we would expect for the carbonyl in this compound. The rest of the signals belong to the aromatic region and fall in line with what we would expect for these derivatives, despite the fact that all of these carbons now have a bromine attached directly to them.

Since the NMR does not provide as much evidence about the identity of this compound, mostly on account of having no aromatic protons, the compound was also tested in a GC/MS. The spectra can be found below.

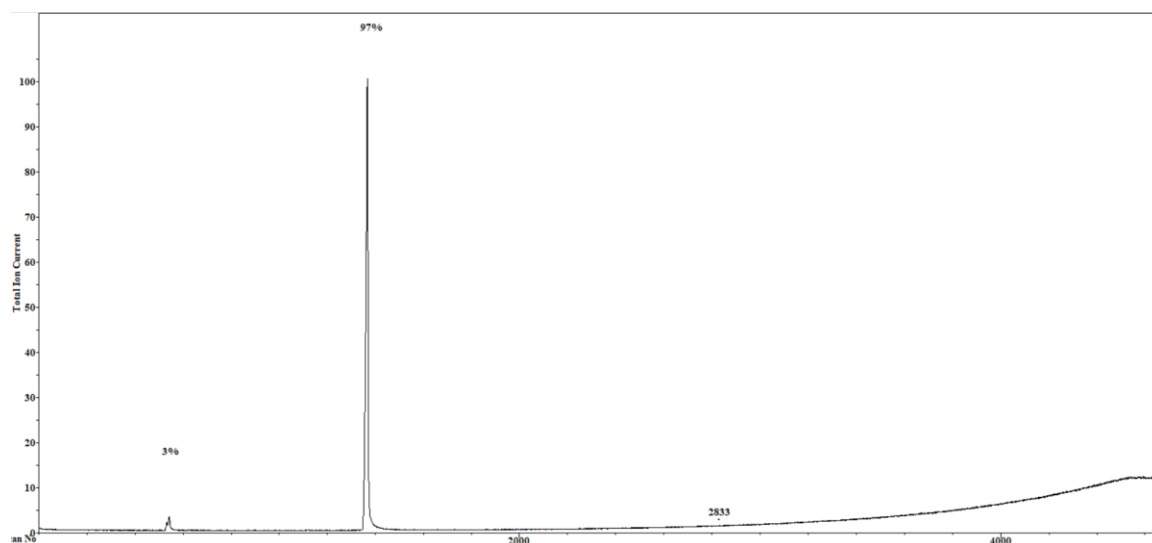


Figure 61. Total ion chromatogram for compound 10. Relative integrations are given above the peaks.

The total ion chromatogram for this compound gives one major peak, and a smaller signal that bears two peaks. The relative integration for the major peak is 97% suggesting it is the major product, while the other compounds are much smaller in abundance. This is complemented from the integration of the aromatic signals in the  $^1\text{H}$  NMR versus the

N-H signal. Next we looked at the MS spectrum for each of these peaks to learn their identities.

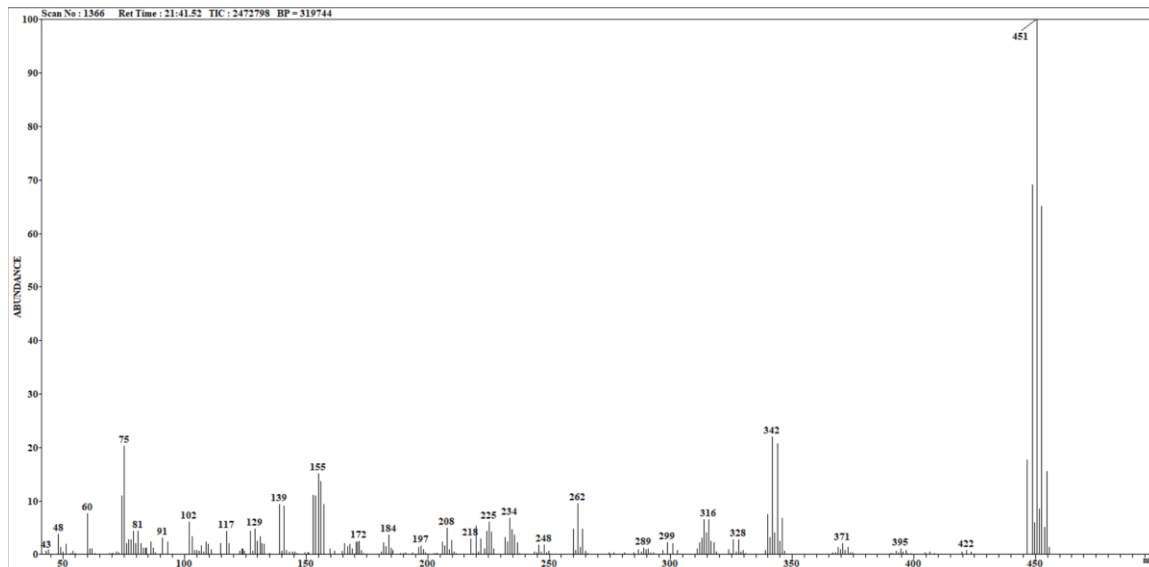


Figure 62. Mass spectrum for the largest peak in the TIC.

The major compound gives a  $m/z$  of 451, which matches the molecular mass we would expect for a benzoxazolone compound with four bromines instead of aromatic protons.

The fragmentation pattern also provides strong evidence that bromines are present, as the abundance of bromine 79 and 81 isotopes is about 50/50, which means we would expect signals that are 2  $m/z$  units apart. Using probability, the 451 ion belongs to the most abundant compound where there is an equal distribution of 79 and 81 bromine isotopes.

Then the next set of peaks which are slightly less abundant belong to the case where there are 3 of one type of isotope, and then only 1 of the other. Then the next set of peaks belong to the compounds where all the bromines are the same isotope.

There are many other fragments in this spectrum, but it is difficult to determine the identity of many of these. Given that the molecular weight of bromine atoms are either 79 or 81, we would expect to see a peak corresponding to  $m/z = 370$  or  $372$ , where one of the bromine atoms were removed, and so on as more bromine atoms fall off. While there are some peaks corresponding to these mass to charge ratios, they are at quite low intensity, so it is difficult to use this data with confidence. Next we'll look at the impurities.

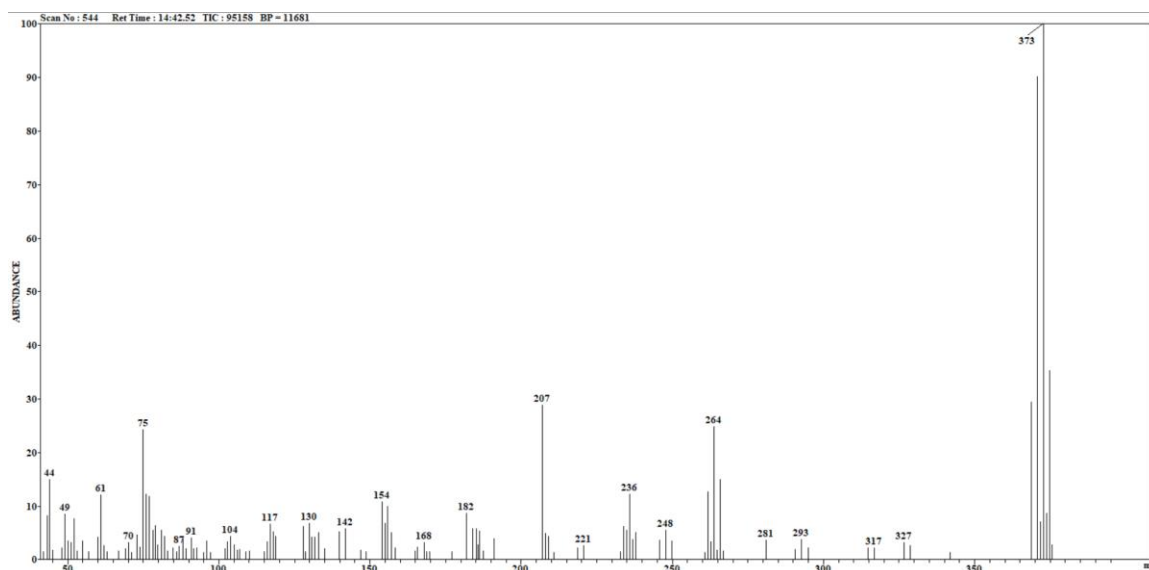


Figure 63. Mass spectrum for the second largest peak in the TIC.

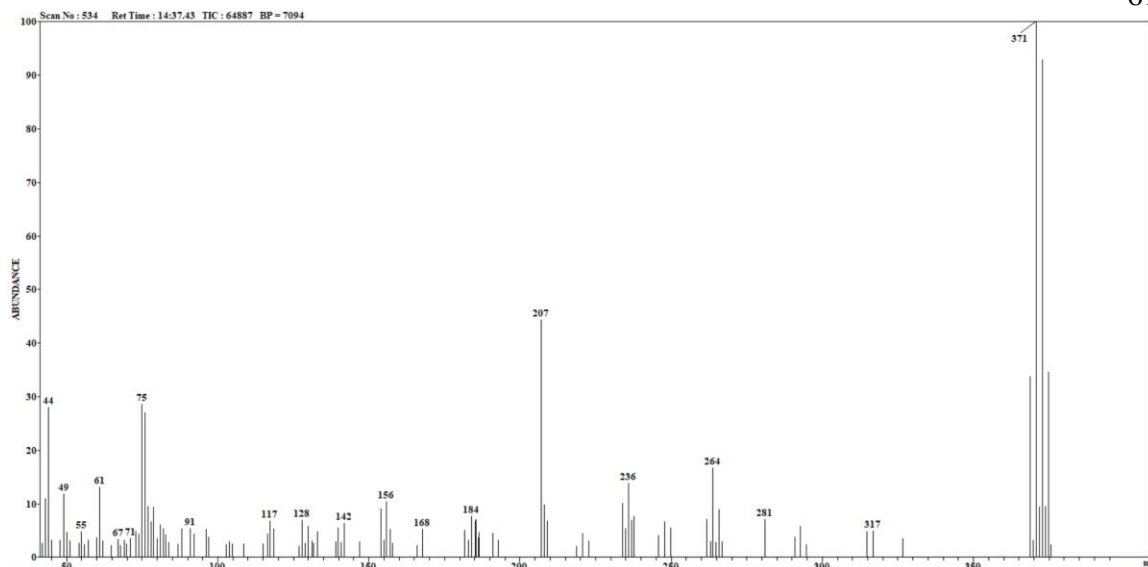


Figure 64. Mass spectrum for the third largest peak in the TIC.

Again the impurities gave one lump signal with two peaks as can be seen in the TIC.

These two peaks have the major ions of 371 and 373 m/z. These both match what would be expected for a benzoxazolone compound with 3 bromines and 1 aromatic proton. This means that this one signal belongs to just one compound, however two peaks can be seen. It appears that the heavier 373 m/z isotope may have a large enough difference in boiling point compared to the lighter 371 m/z isotope to make these signals separate out, at least with the method used to acquire this spectrum. Again, the fragmentation patterns can be explained similar to the major compound. Since there are a total of three bromines there is equal probability that you could have 2 heavy isotopes and 1 light, or 2 lights and 1 heavy, this gives rise to the two peaks of the same abundance at 371 and 373 m/z. Then the next two outer peaks belong to the compounds that have either 3 heavy or 3 light isotopes of bromine.

Overall, the identity of the compound of interest and the impurities make sense in light of these GC/MS data. It makes sense that the major product was saturated with bromines, with some tribromo compounds left over that did not fully react, given the reaction conditions. In addition, it is worth comparing the elution order of these compounds. GC/MS retention times are largely determined by boiling point, and here we see the tetrabromo compound, which has a higher molecular weight and therefore a higher boiling point, elute much later than the compounds with a lower molecular mass, and a lower boiling point.

### Compound 11

A  $^1\text{H}$  and  $^{13}\text{C}$  spectrum were acquired for this compound, which can be seen below.

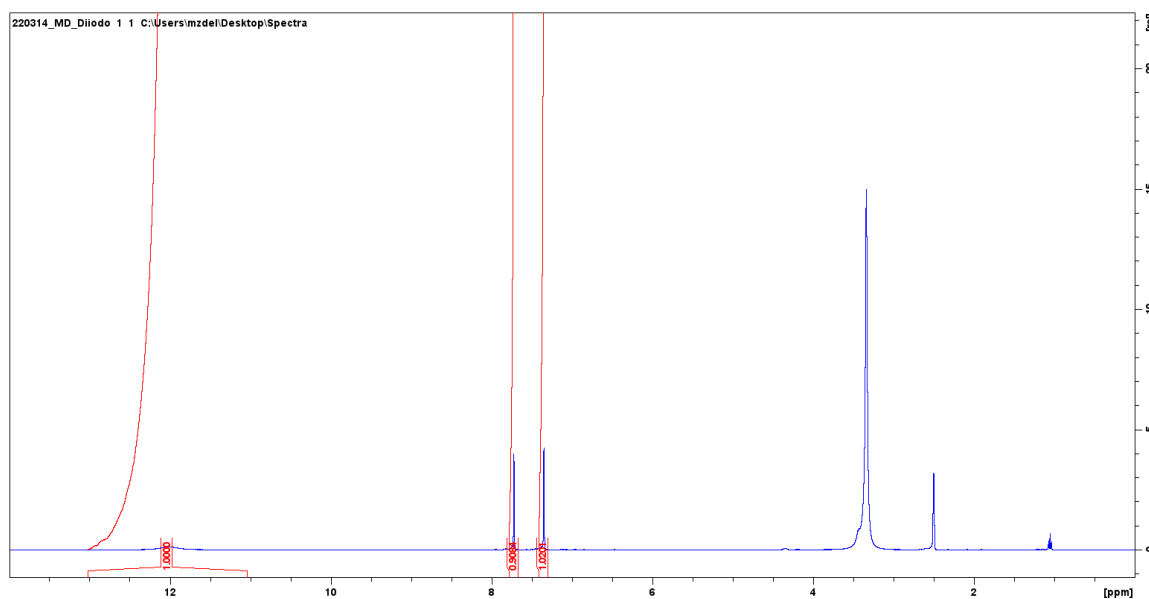


Figure 65. Full  $^1\text{H}$  Spectrum for compound 11. Peak at 3.34 is due to water.

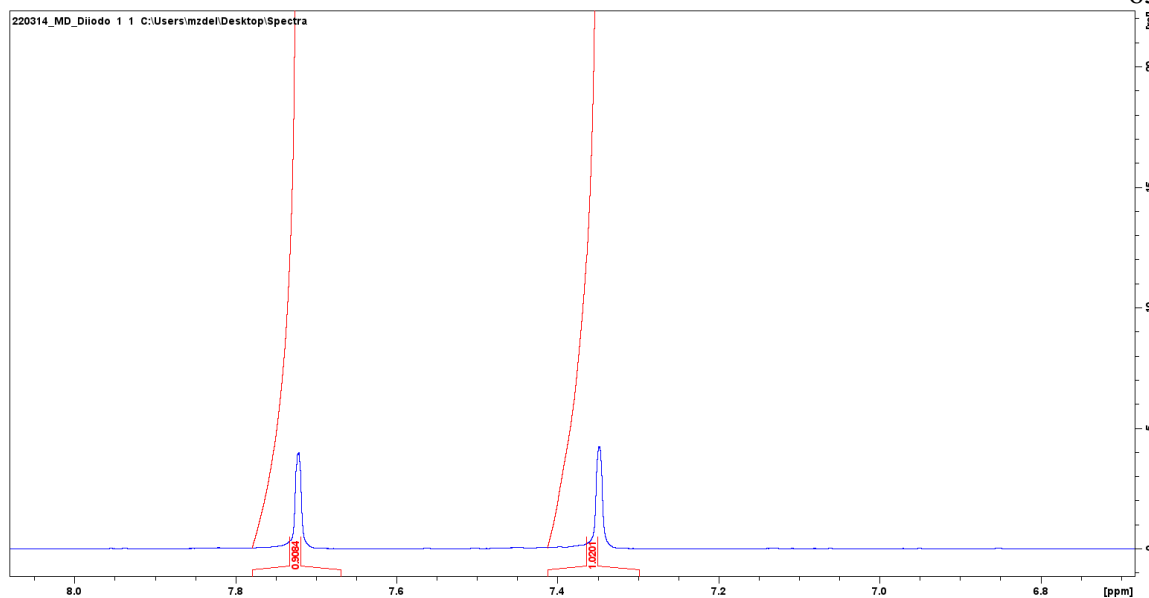


Figure 66. Aromatic region of  $^1\text{H}$  Spectrum for compound 11.

In the  $^1\text{H}$  NMR spectrum we acquire three signals that integrate to 3H, which is what we would expect for this compound since two of the aromatic protons were substituted for iodine. The highest shifted signal lies at 12.01 ppm, which is within the range expected for these compounds. The aromatic singlets shifted at 7.72 and 7.35 ppm. The fact that they are both singlets suggests that the iodine atoms substituted in an alternating pattern so either at the 4 and 6 positions or the 5 and 7 positions. Either one could be possible in theory so further analysis is needed, which will be discussed later.

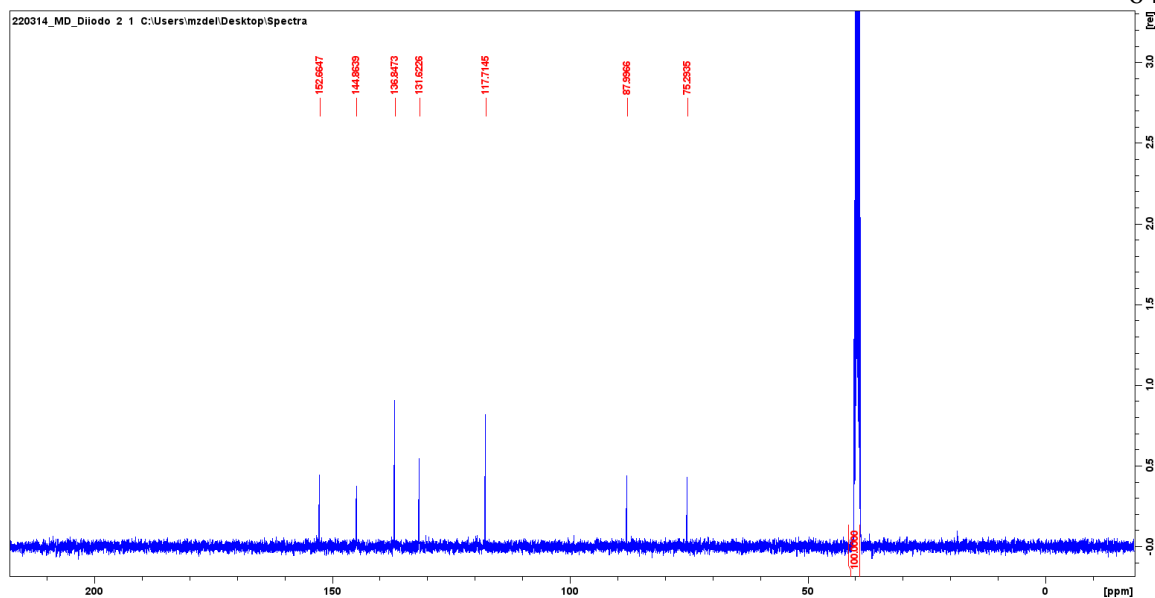


Figure 67. Full  $^{13}\text{C}$  Spectrum for compound 11.

The  $^{13}\text{C}$  spectrum gives a total of seven signals, which is expected for this compound. The highest shifted signal shifted at 152.7, which matches what we would expect for the carbonyls in these derivatives. The rest of the signals belong to the aromatic ring. There is some notably different behavior for the signals in this spectrum when compared to the other derivatives, however. We have two lowly shifted signals at 88.0 and 75.3 ppm, which is remarkably low for aromatic carbons. However, it is well documented that iodine can cause carbons signals to shift much lower than what would be expected. Therefore, it is likely that these are the two carbons bearing an iodine atom.



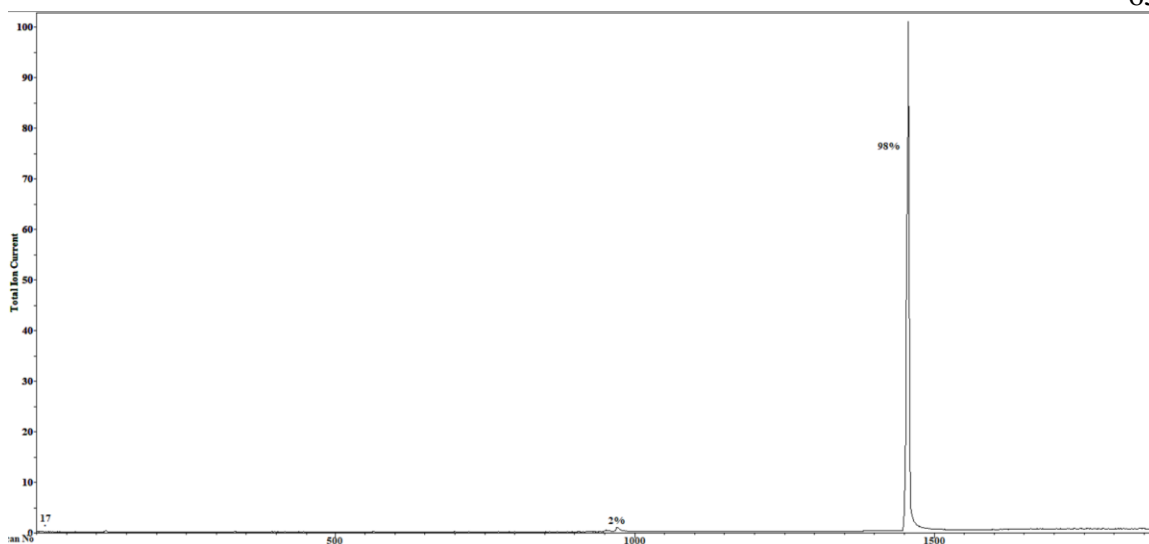


Figure 68. Total ion chromatogram for compound 11. Relative integrations are given above the peaks.

Above is the total ion chromatogram for this compound. One major signal can be seen with a minor signal with only 2% of relative integration. To verify the identity of these peaks, mass spectra were recorded.

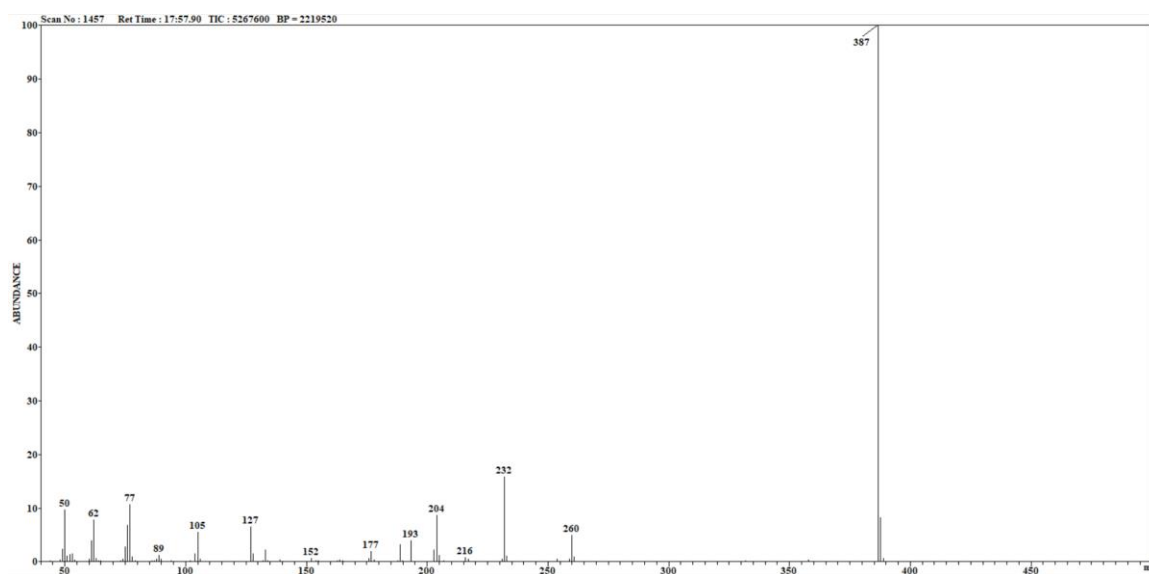


Figure 69. Mass Spectrum for the largest peak in the TIC.

As can be seen in Figure 69 the largest peak in the TIC gives a the most intense fragment at  $m/z = 387$ . This matches the molecular mass for a benzoxazolone molecule with two iodine atoms substituted for hydrogens. No significant fragmentation pattern is observed at this peak, which is typical for iodine which, unlike bromine, does not have any isotopes occurring in significant abundance. Another important fragment can be seen at  $m/z = 260$ , which is 127 units lower than the molecular ion. This matches what would be expected for iodine leaving the molecule, which helps to support the idea that we have iodine in this molecule. In addition, a small peak can be seen at  $m/z = 133$ , which is another 127 units lower than 260, which suggests a second iodine left this molecule.

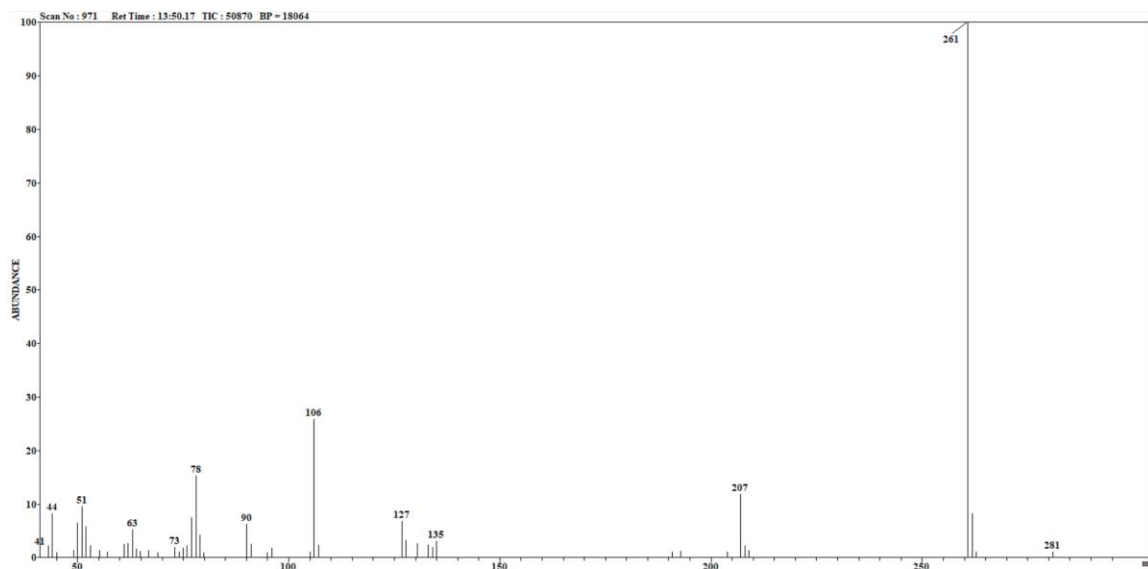


Figure 70. Mass spectrum for the second largest peak in the TIC.

The impurity in this sample has the most intense fragment with a mass to charge ratio of 261, which matches the molecular weight for benzoxazolone with one iodine atom. Given

the reaction conditions, it makes sense that perhaps some compound did not fully convert and only had one iodine added instead of two.

Overall given this analysis, it is apparent that the identity of this sample is a diiodo benzoxazolone, however the possibility of isomers still needs to be addressed. Perhaps the best way to solve this issue is to obtain crystals for X-ray crystallography.

Unfortunately, these compounds have proved to be very difficult to crystallize, so this could not be done during this project. In lieu of a crystal structure, the carbon NMR's can be overlapped from our compound and those seen in literature, which affords strong evidence that the compound we isolated has iodines in the 5 and 7 positions. The only difference is a 0.1 ppm shift in one of the signals, the rest line up exactly. The raw data can be seen in the Appendix.

### **Conclusion**

In this work we have found a brand-new route of synthesis for benzoxazolone and its derivatives. This provides numerous benefits. First, the reaction conditions involve a simple solvent system, and just one equivalent of potassium periodate, which is a widely available, cheap, and green reagent. The reaction requires no heat, special atmosphere, etc. which makes for a very convenient synthesis of these compounds from 2H-1,4-Benzoxazine-2,3(4H)-dione derivatives. Second, this new route of synthesis allows benzoxazolone derivatives to be made from isatin or aniline derivatives, as benzoxazine-2,3(4H)-dione compounds can be readily made from isatin via a Baeyer-Villiger oxidation, and isatin can be readily synthesized from aniline via a Sandmeyer method. The typical route of synthesis seen in the literature is from aminophenol derivatives, so it

is now possible to access benzoxazolone derivatives from different starting materials, which may make some syntheses easier or even possible. Given the versatility of benzoxazolone, especially in the field of medicine, we hope that this route of synthesis proves useful.

In the future we would like to perform additional experiments to explore the mechanism of this reaction. In doing so, it is entirely possible that the conditions could be optimized further, and it is possible that the reaction could be applied to other scenarios as well, outside of the synthesis of benzoxazolone. For example, we would like to try synthesizing benzothiazolone and its derivatives through 2H-1,4-Benzothiazine-2,3(4H)-dione derivatives. We hypothesize this should be possible given its chemical similarity to 2H-1,4-Benzoxazine-2,3(4H)-dione. If this would prove successful, then this reaction scheme would provide convenient access to another selection of very important medicinal compounds.

## **Materials and Methods**

### **Instrumentation**

All NMR spectra were acquired from a Bruker Ascend 400 MHz machine. All the spectra were measured in  $d_6$ -DMSO. Calibration was performed by setting the DMSO solvent signal to 2.50 ppm in  $^1\text{H}$  NMR spectra and 39.51 ppm in  $^{13}\text{C}$  NMR spectra.

All GC/MS spectra were acquired from an Agilent 7890B GC System with an Agilent GC/MSD 5977B.

## Synthetic Methods

All the reagents were used from the manufacturer without further purification.

### Preparation of Benzoxazolone and Derivatives (Using Oxone and KI)

To a 50 mL Round bottom flask with a stir bar add 1 mmol of 2H-1,4-Benzoxazine-2,3(4H)-dione (163mg), 0.1 equivalents of potassium iodide (16.6mg), 1.2 equivalents of Oxone (744mg), 7 mL of Acetonitrile, and 21 mL of DI Water. Stir at room temperature overnight.

Extract from the filtrate using 3 portions of 10 mL of ethyl acetate. Combine the organic portions and wash with sodium thiosulfate solution (5%) until excess iodine is removed. Wash the organic layer with 15 mL of water followed by 15 mL of brine. Dry over magnesium sulfate, and filter. Concentrate to acquire the product.

### Preparation of Benzoxazolone and Derivatives (Using Potassium Periodate)

To a 50 mL Round bottom flask with a stir bar add 1 mmol of 2H-1,4-Benzoxazine-2,3(4H)-dione (163mg), 1 equivalent of potassium periodate (230mg), 7 mL of Acetonitrile, and 21 mL of DI Water. Stir at room temperature overnight.

Extract from the filtrate using 3 portions of 10 mL of ethyl acetate. Combine the organic portions and wash with sodium thiosulfate solution (5%) until excess iodine is removed.

Wash the organic layer with 15 mL of water followed by 15 mL of brine. Dry over magnesium sulfate, and filter. Concentrate to acquire the product.

#### Preparation of 2H-1,4-Benzoxazine-2,3(4H)-dione and Derivatives

To a 100 mL beaker with a stir bar add 19 mL H<sub>2</sub>SO<sub>4</sub>, 1 mL H<sub>2</sub>O, and 3.25g Potassium Persulfate (12 mmol). Cool the mixture to 0°C. Gradually add 10 mmol of the isatin derivative over 30 minutes. Stir the reaction mixture for 1 hour, still keeping the temperature at 0°C. Add the reaction mixture to 200 mL of ice and vacuum filter. Wash with water. Product will be on the funnel.

#### Preparation of isatin and derivatives

To a 500 mL Erlenmeyer flask with a stir bar add 88.8 mmol of aniline derivative, 22.2g hydroxylamine HCl (320 mmol), 100.8g sodium sulfate, 620 mL H<sub>2</sub>O, 5 mL 12 M HCl. Stir briefly, then add 17.6g chloral hydrate (106 mmol). Stir for 24 hours at 55°C. Cool to room temperature and filter.

Add the collected compound in portions to 45 mL H<sub>2</sub>SO<sub>4</sub> at 55°C. Heat to 80°C for 30 minutes, then cool to room temperature. Pour into 225 mL ice and place in cold water bath for 30 minutes. Filter, wash with water. Product will be on the funnel.

## Bibliography

- Hwang, J. et al. (2000). Synthesis and characterization of photoconducting non-linear optical polymers containing indole-benzoxazole moiety. *Polymer*, Vol. 42(2001), p. 3023-3031.
- Kakkar S. et al. (2018). Benzoxazole derivatives: design, synthesis, and biological evaluation. *Chemistry Central Journal*, Vol. 12(92).
- Michael, K. et al. Preparation of heterocyclalkylbenzazolidinones as muscarinic M1 and M4 agonists. *PCT Int. Appl.* (2003), 90 pp. CODEN:PIXXD2.
- Nachman, R (1982). Convenient preparation of 2-benzoxazolinones with 1,1-carbonyldiimidazole. *Journal of heterocyclic chemistry*, 1982, Vol. 19(6), p. 1545-1547.
- Narender, N. et al. (2002). Regioselective oxyiodination of aromatic compounds using potassium iodide and oxone®, *Synthetic Communications*, 32:15, 2319-2324, DOI: 10.1081/SCC-120006002.
- Soyer, Z. et al. (2014). Synthesis and antioxidant activity studies of some 5-chloro-3-substituted 2(3H)-Benzoxazolone derivatives. *Asian Journal of Chemistry*, Vol. 26(19), p. 6642-6646.
- Ucar, H. et al. (1998). Synthesis and anticonvulsant activity of 2(3H)-Benzoxazolone and 2(3H)-Benzothiazolone derivatives. *J. Med. Chem.*, Vol. 41(7), p. 1138-1145.
- Varma, R. and Kapoor, A. (1977). New methods for the synthesis of Benzoxazolin-2-ones. *Current Science*, Vol. 46(22), p. 779-780.

## Appendix

### Spectroscopy Data

#### Compound 1 (Sample MD298)

$^1\text{H}$  NMR (DMSO, 400 MHz):  $\delta$  11.62 (d, 1H, NH), 7.26 (d, 1H,  $J = 8.0$  Hz, 7-H), 7.03-7.17 (m, 3H).

$^{13}\text{C}$  NMR (DMSO, 100 MHz):  $\delta$  154.4 (C-2), 143.3 (C-7a), 130.3 (C-3a), 123.8 (C-5), 121.8 (C-6), 109.8 (C-4), 109.5 (C-7).

Table 9.  $^1\text{H}$   $^{13}\text{C}$  HSQC data for Compound 1.

$^1\text{H}$ Signal	$^{13}\text{C}$ Signal
7.13	123.8
7.07	121.8
7.08	109.8
7.26	109.5

Table 10.  $^1\text{H}$   $^{13}\text{C}$  HMBC data for Compound 1.

$^1\text{H}$ Signal	$^{13}\text{C}$ Signal
11.62	154.5
11.62	143.6
11.62	130.3
7.26	130.3
7.26	123.7
7.08	121.8
7.13	109.5
7.13	130.3
7.07	109.8

Table 11. COSY data for Compound 1.

$^1\text{H}$ Signal	$^1\text{H}$ Signal
11.62	7.26
7.26	7.07

Table 12.  $^1\text{H}$   $^{15}\text{N}$  HMBC data for Compound 1.

$^1\text{H}$ Signal	$^{15}\text{N}$ Signal
11.62	111.9



Table 13. NOESY data for Compound 1.

11.62	7.08
-------	------

## MS

Mass EI m/z: 135(100), 91(17), 79(44), 52(28).

Compound 2 (Sample MD333)

$^1\text{H}$  NMR (DMSO, 400 MHz):  $\delta$  12.15 (s, 1H, NH), 7.34 (dd, 1H,  $J = 8.1, 0.9$  Hz), 7.30 (dd, 1H,  $J = 8.1, 0.9$  Hz), 7.04 (t, 1H,  $J = 8.1$  Hz).

$^{13}\text{C}$  NMR (DMSO, 100 MHz):  $\delta$  153.7, 143.5, 130.6, 126.5, 123.1, 108.7, 100.9.

Compound 3 (Sample MD357)

$^1\text{H}$  NMR (DMSO, 400 MHz):  $\delta$  11.84 (s, 1H, NH), 7.25 (m, 1H), 7.20-7.23 (m, 2H).

$^{13}\text{C}$  NMR (DMSO, 100 MHz):  $\delta$  154.1, 142.5, 132.1, 124.3, 115.3, 112.5, 111.2.

Compound 4 (Sample MD362)

$^1\text{H}$  NMR (DMSO, 400 MHz):  $\delta$  11.80 (s, 1H, NH), 7.58 (d, 1H,  $J = 1.9$  Hz, 7-H), 7.32 (dd, 1H,  $J = 8.3, 1.9$  Hz, 5-H), 7.05 (d, 1H,  $J = 8.3$  Hz, 4-H).

$^{13}\text{C}$  NMR (DMSO, 100 MHz):  $\delta$  154.0, 144.0, 129.8, 126.4, 113.0, 112.7, 111.2.

Compound 5 (Sample MD331)

$^1\text{H}$  NMR (DMSO, 400 MHz):  $\delta$  11.99 (s, 1H, NH), 7.25-7.31 (m, 1H), 7.10 (d, 1H,  $J = 1.3$  Hz), 7.09 (s, 1H).

$^{13}\text{C}$  NMR (DMSO, 100 MHz):  $\delta$  153.3, 141.2, 131.4, 125.2, 124.5, 109.2, 100.8.

Compound 6 (Sample MD303)

$^1\text{H}$  NMR (DMSO, 400 MHz):  $\delta$  11.90 (s, 1H, NH), 7.29 (d, 1H,  $J = 8.5$  Hz), 7.14 (s, 1H), 7.10 (d, 1H,  $J = 8.5$  Hz).

$^{13}\text{C}$  NMR (DMSO, 100 MHz):  $\delta$  154.2, 142.1, 131.7, 127.7, 121.5, 110.7, 109.8.

Compound 7 (Sample 296)

$^1\text{H}$  NMR (DMSO, 400 MHz):  $\delta$  11.84 (s, 1H, NH), 7.47 (d, 1H,  $J = 2.0$  Hz, 7-H), 7.19 (dd, 1H,  $J = 8.3, 2.0$  Hz, 5-H), 7.09 (d, 1H,  $J = 8.3$  Hz, 4-H).

$^{13}\text{C}$  NMR (DMSO, 100 MHz):  $\delta$  154.1, 143.7, 129.4, 125.7, 123.6, 110.7, 110.2.

Compound 8 (Sample MD371)

$^1\text{H}$  NMR (DMSO, 400 MHz):  $\delta$  11.47 (s, 1H, NH), 7.09 (s, 1H, 7-H), 6.91-6.97 (m, 2H), 2.30 (s, 3H,  $\text{CH}_3$ ).

$^{13}\text{C}$  NMR (DMSO, 100 MHz):  $\delta$  154.6 (C-2), 143.5 (C-3a), 131.3 (C-6), 127.8 (C-3a), 124.0 (C-5), 110.0 (C-7), 109.3 (C-4), 20.9 ( $\text{CH}_3$ ).

Table 14.  $^1\text{H}$   $^{13}\text{C}$  HSQC data for Compound 8.

$^1\text{H}$ Signal	$^{13}\text{C}$ Signal
7.09	110.0
6.94	109.3
6.94	124.0
2.30	20.9

Table 15.  $^1\text{H}$   $^{13}\text{C}$  HMBC data for Compound 8.

$^1\text{H}$ Signal	$^{13}\text{C}$ Signal
11.47	154.6
11.47	143.5
11.47	127.8
2.30	110.0
2.30	124.0
2.30	131.4
6.94	131.4
6.94	143.5
6.95	127.8
7.09	124.0
7.09	127.9
7.09	143.5

Table 16. COSY data for Compound 8.

$^1\text{H}$ Signal	$^1\text{H}$ Signal
11.47	7.09

Table 17.  $^1\text{H}$   $^{15}\text{N}$  HMBC data for Compound 8.

$^1\text{H}$ Signal	$^{15}\text{N}$ Signal
11.47	110.0

Compound 9 (Sample MD359)

$^1\text{H}$  NMR (DMSO, 400 MHz):  $\delta$  11.47 (br, 1H, NH), 7.14 (s, 1H), 6.97 (m, 2H), 2.60 (q, 2H,  $J = 7.6$  Hz), 1.16 (t, 3H,  $J = 7.5$  Hz).

$^{13}\text{C}$  NMR (DMSO, 100 MHz):  $\delta$  154.6, 143.5, 137.9, 128.0, 122.9, 109.3, 108.9, 28.0, 15.9.

Compound 10 (Sample MD268F)

$^1\text{H}$  NMR (DMSO, 400 MHz):  $\delta$  12.68 (s, 1H, NH).

$^{13}\text{C}$  NMR (DMSO, 100 MHz):  $\delta$  152.7, 141.4, 132.2, 121.6, 119.0, 104.5, 104.1.

MS

Mass EI m/z: 451(100), 342(22), 155(15), 75(21).

Compound 11 (Sample MD\_Diiodo)

$^1\text{H}$  NMR (DMSO, 400 MHz):  $\delta$  12.01 (s, 1H, NH), 7.72 (s, 1H), 7.35 (s, 1H).

$^{13}\text{C}$  NMR (DMSO, 100 MHz):  $\delta$  152.7, 144.9, 136.8, 131.6, 117.7, 88.0, 75.3.

MS

Mass EI m/z: 387(100), 232(16), 77(11).

From Literature for comparison to 11 (Michael et al., 2003)

$^1\text{H}$  NMR (DMSO):  $\delta$  11.96 (br, 1H), 7.71-7.70 (m, 1H), 7.34-7.32 (m, 1H).

$^{13}\text{C}$  NMR (DMSO):  $\delta$  152.6, 144.9, 136.8, 131.6, 117.7, 88.0, 75.3.